

**Cloning and Enzymatic Characterization of *Polysiphonia japonica*
Methionine Dehydrogenase**

By
Emily J. Garrett

A thesis submitted to the Department of Chemistry and Biochemistry at
Mount Allison University in partial fulfillment of the requirements for the
Bachelor of Science degree with Honours in Biochemistry

April 2020

TABLE OF CONTENTS

Abstract	4
Acknowledgements	5
List of Abbreviations.....	6
List of Figures	8
Introduction	10
The Biological Roles of DMSP.....	10
DMSP and the Global Sulfur Cycle	12
DMSP Biosynthesis.....	13
Deamination of methionine and involvement of a <i>Polysiphonia</i> megasynthetase.....	15
Amino Acid Dehydrogenases	17
Materials and Methods	19
Chemicals.....	19
Bioinformatic Analysis of PjMetDH.....	19
Protein quantification	19
Bradford method	19
Gel electrophoresis	20
Transformation of PjMetDH::pET42b(+) into bacterial expression cells	21
Liquid culture of pET28b and pET44a transformed <i>E. coli</i> Top10 culture cells.....	21
Plasmid purification.....	21
Restriction endonuclease digest of purified plasma DNA.....	22
Ligation of the PjMetDH-H ₆ ::pET28b(+) and NUS-PjMetDH::pET44a(+) constructs.....	22
Dephosphorylation of the empty pET44a and pET28b plasmids	23
PCR confirmation of positive colonies.....	23
Heat Shock Transformation protocol	24
Purification, quantification and restriction endonuclease digest of PjMEtDH-H ₆ ::pET28b Plasmid DNA.....	24
<i>EcoRI</i> -HF digest confirmation of PjMetDH-H ₆ insert into pET28b.....	25
PCR analysis of PjMetDH-H ₆ ::pET28b construct	25
Protein Expression trial 1	26
Electrotransformation of PjMetDH::pET42b and pGEX-4T-3 into <i>E. coli</i> RIPL cells ...	26
Day cultures of <i>E. coli</i> RIPL transfected with PjMetDH::pET42b.....	26
Harvesting and homogenization of <i>E. coli</i> RIPL cells	27

Protein purification	27
Desalting of purified GST-PjMetDH.....	28
Thrombin cleavage	28
Kinetic assay of the impure, cleaved GST-PjMetDH.....	28
Purification of PjMetDH from GST	28
Desalting of cleaved PjMetDH.....	29
Protein expression trial 2	29
Thrombin cleavage	29
Desalting of purified, cleaved PjMetDH: Nanosep concentrator.....	29
Desalting of purified, cleaved PjMetDH: desalting column	29
Desalting of purified, cleaved PjMetDH: dialysis cassette.....	30
Glutathione colorimetric assay	30
Results.....	31
Phylogenetic relationship of PjMetDH and other amino acid dehydrogenases	31
Cloning of PjMetDH constructs	34
Protein expression trial 1	42
Protein expression trial 2.....	46
Discussion	49
Future directions.....	52
References	53

Abstract

Dimethylsulfoniopropionate (DMSP) is an organosulfur molecule produced by many marine algae, bacteria, and plants. The physiological roles of this metabolite include acting as an osmolyte, antioxidant, predator deterrent and cryoprotectant. DMSP is linked to the global sulfur cycle as the breakdown product of DMSP; dimethyl sulfide (DMS) by marine bacteria and algae contributes a substantial amount of sulfur to the global sulfur cycle. The breakdown products of DMSP have also been shown to be involved in climate regulation by acting as cloud condensing nuclei. There exist three distinct DMSP biosynthetic pathways, one in algae, bacteria and higher plants. In marine algae, the four-step enzymatic pathway begins with the reversible transamination of methionine to 4-methylthio-2-oxobutyrate (MTOB) by methionine aminotransferase. The first step of the DMSP biosynthetic pathway has been extensively studied in marine algae such as *Ulva*, leaving this step, in other species such as *Polysiphonia*, poorly characterized. A ‘megasyntetase’ multi-domain fusion protein discovered in *Polysiphonia* is believed to contain a putative methionine specific amino acid dehydrogenase (PjMetDH) domain from the Glu/Val/Leu/Phe dehydrogenase family that is hypothesized to be involved in catalyzing the first step of the DMSP biosynthetic pathway.

The objective of the present study is to validate the identity of this putative methionine dehydrogenase by cloning, expressing, purifying, and enzymatically characterizing a recombinant methionine dehydrogenase. The methionine dehydrogenase was successfully cloned in one of the original three gene constructs, expressed and partially purified. The GST affinity tag was successfully cleaved from the methionine dehydrogenase portion of the fusion protein, however the two could not be separated due to solubility issues that were encountered. Future studies of the putative methionine dehydrogenase will include completing the purification and enzyme characterization as well as cloning the two unsuccessful gene constructs.

Acknowledgements

Firstly, I would like to thank Dr. Jeffrey Waller for acting as my supervisor for the last year and a half. The skills and knowledge that I have acquired over the course of working in the Waller lab will be of tremendous value in future research endeavors. Additionally, I would like to thank Dr. Jillian Rourke for acting as my second reader, you have been an exceptional addition to the Mount Allison Chemistry and Biochemistry department and a great role model. I would also like to thank Dr. Tyson MacCormack for hosting the Waller lab during the seemingly never-ending Gairdner renovations as well as for providing guidance as it pertains to further education in the field of biochemistry.

Secondly, I would like to thank the members of Team DMSP, Brian Beardsall and Mireille Savoie. Brian, you have been a fantastic lab mate, your kindness and willingness to help have been much appreciated. Mireille, your knowledge of the Waller lab and willingness to answer even the silliest of questions has been a valued contribution to this work.

To all the faculty and staff of the Mount Allison Chemistry and Biochemistry, and the Biology departments, thank you for the knowledge and experience you have allowed me to gain and the memories you have facilitated over these last four years of my undergraduate degree.

Finally, I would like to thank NSERC, CFI, NBIF and Mount Allison for funding this project and making this research possible.

List of Abbreviations

BGG	Bovine γ -globulin
BSA	Bovine serum albumin
CNN	Cloud-condensing nuclei
DMS	Dimethylsulfide
DMSHB	4-Dimethylsulfonio-2-hydroxybutyrate
DMSO	Dimethyl sulfoxide
DMSP	Dimethylsulfoniopropionate
DTT	Dithiothreitol
EDTA	Ethylenediaminetetraacetic acid
FAD	Flavin adenine dinucleotide
GST	Glutathione <i>S</i> -transferase
H ₆	Hexahistidine
IPTG	Isopropyl β - <i>D</i> -1-thiogalactopyranoside
LB	Lysogeny broth
Met	Methionine
Met DH	Methionine dehydrogenase
<i>D</i> -MTHB	<i>D</i> -Methylthiohydroxybutyrate
MT	MTHB <i>S</i> -Methyltransferase
MTOB	Methylthiooxobutyrate
NADH	Nicotinamide adenine dinucleotide
NADPH	Nicotinamide adenine dinucleotide phosphate
NBE	Non-binding elute

OD	Optical density
PAGE	Polyacrylamide gel electrophoresis
PBS	Phosphate buffered saline
PCR	Polymerase chain reaction
PLP	Pyridoxal-5'-phosphate
SOC	Super optimal broth with catabolite repression
SDS	Sodium dodecyl sulfate
SAM	<i>S</i> -adenosyl methionine
SMM	<i>S</i> -methyl methionine
TAE	TRIS-acetate-EDTA buffer
TRIS	Tris(hydroxymethyl)aminomethane
v/v	Volume / volume
V	Volts
w/v	Weight / volume

List of Figures

Figure 1: Chemical structure of dimethylsulfoniopropionate (DSMP).

Figure 2: Schematic of the three known mechanisms of DMSP production.

Figure 3: Reaction scheme for the deamination of amino acids.

Figure 4: Structure of the *Polysiphonia* 'DMSP synthetase' megasynthetase fusion protein.

Figure 5: The DMSP biosynthetic pathway in marine algae.

Figure 6: Neighbour-joining phylogenetic tree of PjMetDH and other amino acid dehydrogenase enzymes.

Figure 7: Multiple sequence alignment of PjMetDH protein sequence compared to other amino acid dehydrogenases from the Glu/Leu/Phe/Val dehydrogenase family.

Figure 8: Low-melt agarose (1.2% (w/v) in TAE) electrophoresis analysis of the restriction endonuclease digest of the pET44a and pET28b vectors and the PjMetDH::pET42b constructs.

Figure 9: Agarose (1.2% (w/v) in TAE) gel electrophoresis analysis of purified DNA products.

Figure 10: Agarose (1.2% (w/v) in TAE) gel electrophoresis analysis of the PCR products for the detection of positive clones.

Figure 11: Agarose (1.2% (w/v) in TAE) gel electrophoresis analysis of *EcoRI* digested PjMetDH-H₆::pET28b constructs.

Figure 12: Agarose (1.2% (w/v) in TAE) gel electrophoresis analysis of the PCR products for the detection of positive clones.

Figure 13: Agarose (0.8% (w/v) in TAE) gel electrophoresis analysis on the PCR products for the detection of positive clones.

Figure 14: Agarose (0.8% (w/v) in TAE) gel electrophoresis analysis of restriction endonuclease digested PjMetDH-H₆::pET28b construct colonies.

Figure 15: SDS-PAGE (10% (w/v)) gel comparison of the soluble and insoluble fractions of the homogenized bacterial overexpression cells.

Figure 16: SDS-PAGE (10% (w/v)) gel analysis of GST-PjMetDH purification.

Figure 17: SDS-PAGE (10% (w/v)) gel analysis of the thrombin cleavage time trial of GST-PjMetDH.

Figure 18: SDS-PAGE (10% (w/v)) gel analysis of GST-PjMetDH purification.

Introduction

Dimethylsulfoniopropionate (DMSP) is an important metabolite produced by many marine algae and some marine bacteria and higher plants (Otte *et al.*, 2004; Yoch, 2002; Curson *et al.*, 2017). This molecule, first discovered in the red algae *Polysiphonia fastigiata* by Challenger and Simpson in 1947 is a tertiary sulfonium compound with zwitterionic characteristics (Challenger and Simpson, 1947; Yoch, 2002). This organosulfur compound plays a key role as an osmoprotectant in marine algae and bacteria as well as being an important part of the global sulfur cycle (Ksionzek *et al.*, 2016; Yoch, 2002). In this research, a putative methionine dehydrogenase (MetDH) identified in a *Polysiphonia japonica* fusion protein that is believed to catalyze the first step of the DMSP biosynthetic pathway, will be investigated. This study aims to clone the *P. japonica* MetDH gene into a bacterial expression host, expressing the MetDH enzyme, and purify it for enzymatic characterization.

The Biological Roles of DMSP

Sulfur is among the many elements essential to life such as oxygen, carbon, hydrogen and nitrogen. This element makes up about 1% of an organism's dry body weight and is a crucial component of biological compounds such as amino acids (methionine and cysteine), coenzymes, metalloproteins, bridging ligands, and sulfolipids (Howarth, 1984). In some marine algae such as dinoflagellates, prymnesiophytes, chrysophytes, chlorophytes, and some bacteria, DMSP is produced in large quantities and evidence suggests that its purpose is to help the organism regulate their internal osmotic environment in their challenging marine environments (Yoch, 2002; Curson *et al.*, 2017). In organisms such as plants and some microorganisms that experience water stress, the production of osmolytes or compatible solutes has been a known mechanism to maintain the proper osmotic tension in their cells (Keller *et al.*, 1999). In marine species, these osmolytes tend to be nitrogen and sulfur containing compounds. DMSP is an example of these sulfur containing compounds (Keller *et al.*, 1999). DMSP's proposed function as an osmoprotectant is largely based on its structural similarities to other osmoprotectants having tertiary sulfur and quaternary ammonium groups; one such example is glycinebetaine (Otte *et al.*, 2004). In some organisms, the production of both DMSP and glycinebetaine has been reported (Blunden *et al.*, 1992; Dickson and Kirst, 1987). The production of both these osmoprotectants is believed to allow the organism flexibility when it comes to environments

that become nitrogen-limiting. Seawater has abundant amounts of sulfate at around 28 mM whereas the concentration of nitrogen in seawater is between 1-10 μM (Keller *et al.*, 1999). Under nitrogen-limiting conditions, it would be unfavourable to produce osmolytes containing nitrogen when it is required for other fundamental processes such as incorporating nitrogen into amino acids for protein synthesis (Keller *et al.*, 1999). In some species of phytoplankton, DMSP can account for up to 50% of the total sulfur in the organism as well as reaching cellular concentrations of up to 100-500 mM DMSP (Keller *et al.*, 1999; Summers *et al.*, 1998).

The production of DMSP has been reported in many species of higher plants, however DMSP has only been recorded at high concentrations in 3 genera of higher plants: *Spartina*, *Saccharum*, and *Wollastonia*. In *Spartina*, the roles of DMSP have been linked to an overall greater ability to tolerate marsh environments, more specifically by acting as an antioxidant (Husband *et al.*, 2012). As well as being an osmoprotectant for some algal species, DMSP that leeches into the surrounding water can readily be metabolized in order to satisfy the sulfur and carbon requirements for the microbes in the area (Yoch, 2002). Other reported biological roles for DMSP include cryoprotection, sulfur detoxification, antioxidant benefits and herbivore deterrence (Otte *et al.*, 2004).

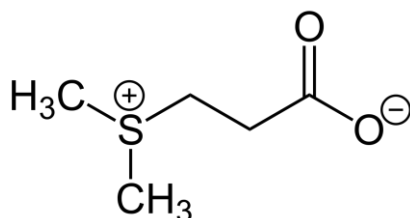


Figure 1: Chemical structure of dimethylsulfoniopropionate (DMSP). The molecule is neutral in charge, its zwitterion characteristics arise due to the positive charge of the sulfur and the negative charge on the carboxyl group.

DMSP and the Global Sulfur Cycle

There is no shortage of sulfur in marine environments (Howarth, 1984). Sulfur can be found in saltwater environments in many forms, notably as sulfate, the second most abundant anion found in saltwater (Keller *et al.*, 1999). In coastal environments where a number of DMSP-producing algae can be found, much of the decomposition occurs via sulfate-reducing bacteria that use sulfate reduction and fermentation to produce energy from decomposition of reduced sulfur products (*e.g.*, hydrogen sulfide, H₂S) (Howarth, 1984). These reduced products in turn lead to intermediate sulfur species that feed into the global sulfur cycle (Jørgensen *et al.*, 2019).

It was long thought that H₂S was responsible for the majority of the sulfur cycling from the ocean to our atmosphere (Robinson and Robbins, 1972; Slatt *et al.*, 1978). However, in 1972, Lovelock *et al.* proposed that since detecting and measuring the presence of this gas had eluded many researchers that perhaps there was another molecule responsible for the cycling of sulfur between sea and air. They proposed that it is in fact DMS that is responsible for the bulk of sulfur flux to the atmosphere. Annually, the degradation of DMSP to DMS by algae and bacteria accounts for approximately 15 million tonnes of sulfur to the global sulfur cycle (Gage *et al.*, 1997). In relative terms, the sulfur contributed to the global sulfur cycle as DMS emissions makes up roughly 50% of the biogenic sulfur flux to the atmosphere (Yoch, 2002). DMS production occurs primarily in the oceans, however flux per unit area is greatest in regions of high decomposition and salinity flux such as in coastal wetlands (Yoch, 2002). DMSP released into the environment can be metabolized via two distinct pathways. The first pathway involves DMSP demethylation to 3-methylpropionate (MMPA) followed by demethylation to 3-mercaptopropionate (MPA) (Taylor and Gilchrist, 1991). A second pathway involves marine algae and bacteria that contain DMSP lyase, an enzyme that will breakdown DMSP to DMS and acrylate (Curson *et al.*, 2017).

When it comes to the environment, DMS has 3 major roles. The first is that DMS is the dominant volatile aerosol released into the global sulfur cycle (Malin, 1996). Secondly, these volatile aerosols are oxidized to acidic products which affect the acid-base chemistry of rainwater (Malin, 1996). Finally, the aerosols methanesulfonic acid and SO₂ that result from the oxidation of DMS act as cloud-condensing nuclei (CCN) (Malin, 1996). The effect of cloud-

condensing nuclei is to promote the formation of clouds over the open ocean as well as creating backscattering of incoming solar radiation. This in turn results in less radiation reaching the Earth's surface, resulting in a decrease in temperature (Yoch, 2002). This leads to a negative feedback system where on sunny days, production of DMSP and the emission of DMS into the atmosphere promotes cloud formation, clouds scatter light and reduce the temperature (Andreae, 1990). Similarly, on a colder day with low light levels, the production of DMS would decrease to allow more solar radiation to reach the surface and increase temperature (Yoch, 2002).

DMSP Biosynthesis

Microalgae and macroalgae are the primary sources of DMSP in the ocean. The primary input into the DMSP pathways is methionine in all organism, including algae, bacteria, and plants, however after methionine, the DMSP biosynthetic pathways differ (Yoch, 2002). The DMSP biosynthetic pathway in the green macroalgae *Ulva intestinalis* (formerly *Enteromorpha intestinalis*) has been elucidated by Gage *et al.* (1997). The researchers demonstrated using *in vivo* isotope labeling that DMSP is produced via a completely unique pathway rather than the pathways found in higher plants (Gage *et al.*, 1997). In this green macroalgae, the pathway begins with methionine as do the rest of the pathways. Methionine is deaminated to form 4-methylthio-2-*D*-oxybutyrate (MTOB) (Gage *et al.*, 1997) (Figure 2). MTOB is then stereospecifically reduced to 4-methylthio-2-*D*-hydroxybutyrate (*D*-MTHB), and finally *D*-MTBH is *S*-methylated to 4-dimethylsulphonio-2-hydroxybutyrate (DMSHB) (Gage *et al.*, 1997). From here, DMSHB is oxidatively decarboxylated to produce the end product DMSP (Gage *et al.*, 1997). The results of this study suggest that the mechanism by which algae produce DMSP evolved independently from the mechanism used by higher plants (Gage *et al.*, 1997).

In higher plants such as *Wollastonia biflora*, the DMSP biosynthetic pathway begins with methionine, as in green algae. In higher plants, the pathway begins with the *S*-methylation of methionine, giving *S*-methylmethionine (SMM) (Stefels, 2000) (Figure 2). This *S*-methylation occurs in tandem with *S*-adenosyl methionine (AdoMet) going to *S*-adenosyl-*L*-homocysteine (AdoHcy) (Stefels, 2000). The next step in this pathway is the transamination and decarboxylation of SMM to produce DMSP-aldehyde and there are no known intermediates between the transamination and decarboxylation steps (Hanson and Gage, 1996). The final step of this pathway is the oxidation of DMSP-aldehyde to DMSP (Stefels, 2000). The enzyme

involved in this final step has been characterized as being similar to the betaine aldehyde dehydrogenase enzyme, these both use NAD^+ as a cofactor (Trossat *et al.*, 1996). Finally, the DMSP synthesis pathway in *Spartina alterniflora* on the surface looks very similar to the mechanism found in *W. biflora*. It diverges only in that there is an intermediate step between SMM and DMSP-aldehyde (Figure 2). SMM is decarboxylated to form DMSP-amine which is then oxidised to DMSP-aldehyde (Kocsis *et al.*, 1998). The enzymes involved here are not known yet, however it is believed that it proceeds via a decarboxylase and an oxidase (Kocsis *et al.*, 1998). The evidence put forward by the authors suggests that each of the three pathways described are unique and have evolved independently from one another (Gage *et al.*, 1997; Hanson *et al.*, 1994; Kocsis *et al.*, 1998).

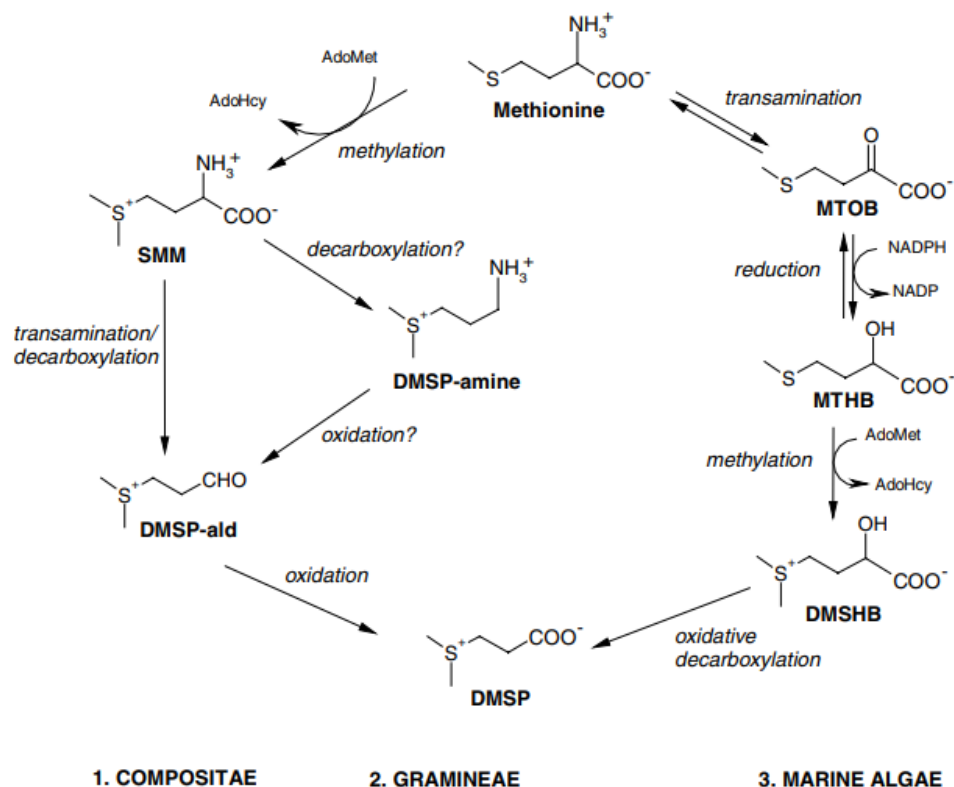


Figure 2: Schematic of the three known mechanisms of DMSP production. 1. Pathway in *W. biflora*. 2. Pathway in *S. alterniflora*. 3. Pathway in *U. intestinalis*. Modified from Stefels (2000)

Deamination of methionine and involvement of a *Polysiphonia* ‘DMSP synthase’ megasynthetase

Although the DMSP biosynthetic pathway has been well characterized in algal species such as *Ulva*, the first step of this pathway in other algal species remains poorly characterised. The deamination of methionine is known to occur via at least 3 mechanisms. The first mechanism occurs via an aminotransferase, Summers *et al* in 1998 reported high affinity toward *L*-methionine and 2-oxoglutarate from methionine aminotransferase extracted from *U. intestinalis*. Aminotransferases, also referred to as transaminases, facilitate the transfer an amino group between amino acids and keto acids in a pyridoxal-5'-phosphate (PLP) dependent manner (Vroon and Israili, 1990) (Figure 3A). The deamination reaction of methionine can also be catalyzed by *L*-amino acid oxidases (Summers *et al.*, 1998). *L*-amino acid oxidases were first described by Zeller and Maritz in 1944, these flavoenzymes catalyze the stereospecific oxidative deamination of *L*-amino acids to their α -keto acid (Figure 3B). Finally, methionine can be deaminated by an amino acid dehydrogenase (Figure 3C).

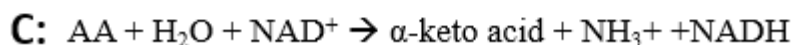
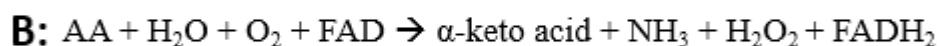
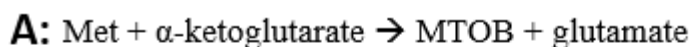


Figure 3: Reaction scheme for the deamination of amino acids. A) Met aminotransferase PLP dependent reaction scheme. B) *L*-amino acid oxidase deamination of Met. C) Amino acid dehydrogenase deamination of Met.

In 2017, J.C. Waller discovered a megasynthetase fusion protein during transcriptome searches of *Polysiphonia* and other algae. This fusion protein, a quadruple domain DMSP synthase appears to contain all four enzymes required for DMSP synthesis. This megasynthetase contains an N-terminal amino acid dehydrogenase (AADH), as well as a methyl transferase (MT), 2-ketoacid reductase (Red), and a class II aldolase (CIIA) (Figure 4). Based on the amino acid dehydrogenase's association with these three other enzymes involved in the DMSP biosynthetic pathway, as well as preliminary phylogenetic searches, it is likely that this amino acid dehydrogenase is methionine-specific and capable of catalysing the first reaction of the DMSP biosynthesis as illustrated in figure 5. Previous work done in the Waller Lab identified methyltransferase-reductase-aldolase fusion proteins in *Ulva* and many other marine algae where researchers have shown that the methyltransferase portion of the fusion protein is the MTHB *S*-methyltransferase of the DMSP biosynthetic pathway (K. Blakeman, 2017; K. Dunning, 2018; F. Hossain, 2018; H. Gale, 2019 and H. Kashiwai, 2019, M. Abergel, D.M. Mills, J.C. Waller, B.D. Beardsall, unpublished data).



Figure 4: Structure of the *Polysiphonia* ‘DMSP synthase’ megasynthetase fusion protein. The discovered fusion protein is made of 4 domains, beginning with an amino acid dehydrogenase domain (AADH) at the N-terminal, followed by methyl transferase (MT), reductase (Red) and aldolase (CIIA) domains.

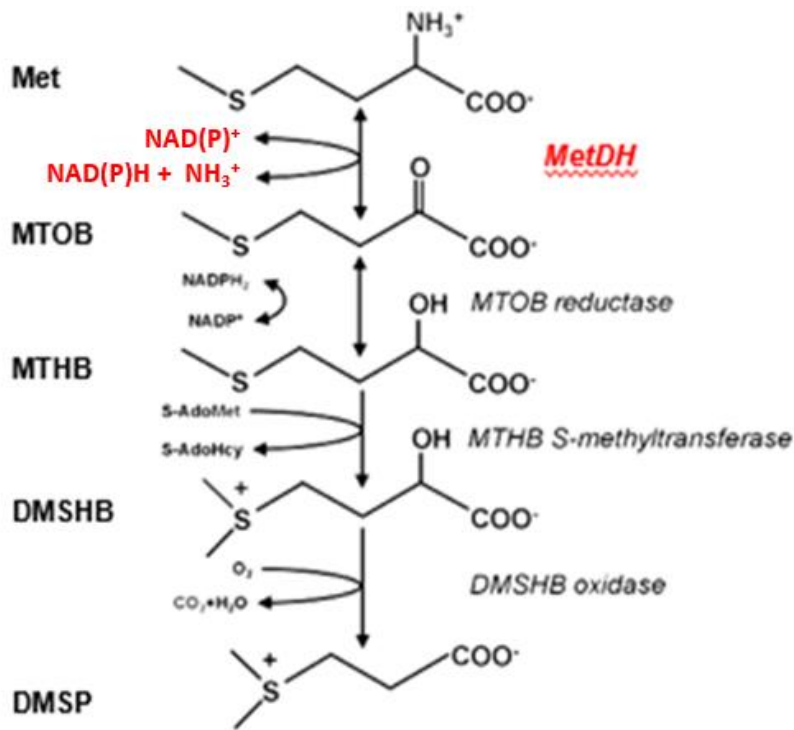


Figure 5: Proposed DMSP biosynthetic pathway in *Polysiphonia*. The DMSP biosynthetic pathway in marine algae showing the hypothesized methionine dehydrogenase and its cofactor in red at the first step. DMSP biosynthesis begins with the reversible oxidative deamination of methionine to 4-methylthio-2-oxobutyrate (MTOB), followed by the reduction of MTOB to 4-methylthio-2-hydroxybutyrate (MTHB), MTHB is irreversibly methylated to 4-dimethylsulfonio-2-hydroxybutyrate (DMSHB) and finally oxidatively decarboxylated to dimethylsulfoniopropionate (DMSP).

Amino Acid Dehydrogenases

Amino acid dehydrogenases participate in a multitude of fundamental processes. At its core, an amino acid dehydrogenase is an enzyme that oxidatively deaminates an amino acid to the cognate keto acid and ammonia while reducing NAD(P)^+ to NAD(P)H (Brunhuber and Blanchard, 1994). Two of the main advantages of using amino acid dehydrogenases as opposed to using transaminases is that amino acid dehydrogenases remove the amino group as ammonia which can then be used by the cell for other purposes, and at the same time reduce NAD(P)^+ to NAD(P)H which can be used in energy requiring steps of metabolism (Brunhuber and Blanchard, 1994). One of the most extensively studied amino acid dehydrogenases is glutamate dehydrogenase. This enzyme is most commonly associated with the ability of plants to maintain their carbon/nitrogen balance during nitrogen assimilation (Mifflin and

Habash, 2002). Many glutamate dehydrogenases have been studied in the literature with variable amino acid specificities as well as variable specificity to NAD⁺ and NADP⁺ (Brunhuber and Blanchard, 1994). In a study by (Wang *et al.*, 2001), a glutamate dehydrogenase was converted to a methionine/norleucine specific dehydrogenase by site-directed mutagenesis. The authors found that in their double mutant, there was no activity of the enzyme in the presence of glutamate and activity with *L*-methionine, *L*-leucine and *L*-norvaline was measurable at pH 7.0, 8.0 and 9.0, a similar pH range as the wild-type glutamate dehydrogenase (Wang *et al.*, 2001). Amino acid dehydrogenases such as leucine, alanine, and glutamate dehydrogenases have been extensively characterized in the literature, however there is still very little known about the specifics involving methionine dehydrogenase (Brunhuber and Blanchard, 1994).

The production of DMSP from methionine has been reported in red algal species such as *Chondria coerulescens* by Chillemi *et al.*, 1990, this provides evidence for the hypothesis that that the enzymes of the fusion protein identified in *Polysiphonia* may contribute to the production of DMSP. The putative amino acid dehydrogenase of the *Polysiphonia* fusion protein is hypothesized to be methionine specific, catalysing the following reversible reaction: $\text{Met} + \text{NAD(P)}^+ + \text{H}_2\text{O} \leftrightarrow \text{MTOB} + \text{NAD(P)}(\text{H}) + \text{NH}_3$. We believe that the first step of the pathway is catalyzed by this methionine dehydrogenase that oxidatively deaminates methionine to MTOB. This hypothesis will be tested by cloning three recombinant variants of the putative methionine dehydrogenase gene. The protein will be expressed in overexpression hosts and purified. The methionine dehydrogenase will be characterized by determining substrate and cofactor specificity pH optima and other enzyme parameters.

Materials and Methods

Chemicals

All buffers were prepared in MilliQ ultrapure water, filtered through a 0.45 µm filter, adjusted to proper pH, and kept at 4°C or 20°C unless otherwise indicated. Chemicals and enzymes were supplied by Sigma-Aldrich, Bioshop Canada, New England Biolabs, GE Lifesciences, Fisher Scientific, MP Biomedical, or BioRad.

Bioinformatic Analysis of PjMetDH

A neighbour-joining phylogenetic tree was produced using the MEGA7 software (version 7.0.26) using the bootstrap consensus tree inferred from 1000 replicates. Evolutionary distances were computed using the number of difference methods were the units are the number of amino acid differences per sequence. The percentage of replicate trees in which the associated taxa clustered together in the bootstrap test are shown next to the branches.

In addition to the phylogenetic tree, a multiple protein sequence alignment was produced comparing the PjMetDH protein sequence to other known amino acid dehydrogenases. The alignment was generated using the T-Coffee software with the Aligns DNA, RNA or Protein default. The alignment output from T-Coffee was input into the BOXSHADE program to generate a grey scale version of the alignment, where highly conserved residues were darkly shaded and non-conserved residues were highlighted in white. Sequences used in both the phylogenetic tree and the multiple protein sequence alignment were retrieved from NCBI, their accession numbers are given in brackets.

Protein quantification

Bradford method

Soluble proteins were quantified using the Bradford method (Bradford, 1976), bovine γ -globulin (BGG) was used to generate a standard curve between concentrations of 0.0-0.4mg/mL. The BioRad Bradford protein dye reagent concentrate was diluted with MilliQ water at a ratio of 1-part dye concentrate 4 parts water, this is denoted as the working strength dye. Protein standards and samples were treated with 250 µL of the working strength dye and incubated in a 96-well clear bottom microplate for 10 minutes, at room temperature before absorbance readings were taken. Absorbance was measured at 595 nm using the Molecular

Devices SpectraMax M3 microplate spectrophotometer. Absorbance data were analyzed using the SoftMax Pro software. A modified version of the Bradford assay was also employed (Zor and Selinger, 1996). This assay also makes use of BGG standards curves, from 0.0 to 0.04 mg/mL and 0.0 to 0.4 mg/mL. Samples were incubated at room temperature from 10 minutes and absorbance was read at 450 and 590 nm. The ratio of the two absorbances (A590/A450) were used to create the standard curve.

Gel electrophoresis

DNA samples were resolved on 0.8 or 1.2% (w/v) agarose-TAE gels, at 120V, in 1X Tris-acetate-EDTA (TAE) buffer, for approximately 30 minutes each. Gels were either prestained with SYBR Safe DNA Gel Stain or stained after electrophoresis with BioShop Safe-T-stain for nucleic acid gel stain. Gels were visualized with the Bio-Rad Molecular Imager VersaDoc MP 4000, data were processed with the Quantity One analysis software by Bio-Rad. DNA ladders used include the 1 kb DNA ladder by GeneDirex (DM010-R500) and the 100 bp DNA ladder by GeneDirex (DM003-R500).

Protein samples were resolved on (10% v/v) Tris-glycine gels at 100V for between 60 and 90 minutes in 1X SDS running buffer (2.5 mM Tris, 9.2 mM glycine, 0.1% (w/v) sodium dodecyl sulfate, all in MilliQ water). Protein ladders include the MBI Rainbow Pre-stained protein ladder (Cat. No. MRPPEVL) and the FroggaBio BLUeye pre-stained protein ladder (Cat. No. PM007-0500K). Before loading, protein samples were denatured by preparing them in 1X Laemmli sample buffer (Laemmli, 1970) and boiling them between 90-100 °C for 5 minutes. Gels underwent two staining protocols. The first involved staining with Coomassie Brilliant Blue R250 (1% (w/v) Coomassie (R-250) Brilliant Blue. 10% (v/v) acetic acid, 50% (v/v) methanol and 40% (v/v) MilliQ water) overnight with agitation and destaining in destain solution composed of 10% (v/v) acetic acid, 40% (v/v) MilliQ water and 50% (v/v) methanol. The second staining method involved staining with SYPRO Ruby protein gel stain (Invitrogen). Manufacturers instructions were followed. The protein gel was incubated in 20 mL SYPRO ruby protein gel stain overnight with agitation, it was then destained in the previously described destain solution. Migration distances of the protein and DNA bands were quantified using the ImageJ program.

Transformation of PjMetDH::pET42b(+) into bacterial expression cells

The 1253 bp long putative *Polysiphonia japonica* methionine dehydrogenase gene (PjMetDH) identified by Dr. Jeffrey Waller, was sent to BioBasic for synthesis into the Novagen's protein overexpression plasmid pET42b(+). The sequence was optimized for expression in bacterial hosts. These optimizations include the removal of restriction endonuclease sites and codon optimization for expression in *Escherichia coli*. The supplied GST-PjMetDH::pET42b(+) plasmid DNA (0.5 µg) was electroporated into 25 µL of *E. coli* DH10β cells using an electrotransformation cuvette and a Micropulser electroporator (BioRad). The time constant reading was 5.70 ms. The cells were recovered in 500 µL Super Optimal Catabolite broth media (SOC) and were left to recover for 45 minutes at 37°C with shaking at 200 rpm. Cells from the recovered cell suspension (50 µL) were plated onto LB agar plates containing 50 µg/µL kanamycin, these were incubated at 37°C overnight. For each construct, a negative control was prepared using the same methods with the exception of using an equal volume of sterile MilliQ water in the place of the plasmid DNA.

Liquid culture of pET28b and pET44a transformed *E. coli* Top10 culture cells

E. coli Top10 cells transformed with pET28b and pET44a from premade glycerol stocks were incubated in 5 mL LB broth with 50 µg/µL kanamycin (pET28b) and 50 µg/µL ampicillin (pET44a) overnight at 37°C, 200 rpm at a 45° incline.

Plasmid purification

Overnight cultures of the PjMetDH::pET42b, pET28b and pET44a *E. coli* cells were centrifuged at 6000 X g for 5 minutes. The supernatant was removed and the cell pellet was processed as outlined by the Monarch[®] Plasmid Miniprep Kit by New England BioLabs protocol with the exception of the addition of a second centrifugation after the addition of wash buffer 2 and the elution of the plasmid DNA in 50 µL warmed (50°C) sterile MilliQ water. The purity and concentration of these plasmid DNA was determined via measurement of the A260/A280 ratio where a pure sample was considered to have a ratio greater than 1.8. A260/A280 ratios were measured using the NanoDrop 1000 spectrophotometer by Thermo Scientific.

Restriction endonuclease digest of purified plasmid DNA

The three plasmid DNA samples; PjMetDH::pET42b, pET28b, and pET44a underwent restriction enzyme digests. Final reaction conditions were 0.5 µg empty vectors pET28b and pET44a or 1 µg of PjMetDH::pET42b, 1X NEB CutSmart Buffer, 1.3 µL of the endonuclease, adjusted to a final volume of 30 µL with the required amount of sterile MiliQ water. The restriction endonuclease combinations that were used were: *NcoI*-HF/*SalI*-HF for the PjMetDH-H6::pET42b construct, *SpeI*-HF/*XhoI*-HF for the NUS-PjMetDH::pET42b construct, *NcoI*-HF/*SalI*-HF for the pET28b plasmid, and *SpeI*-HF/*XhoI*-HF for the pET44a plasmid. The digest was performed at 37°C for 1 hour. The digest products were separated by resolving them on a 1.2% (w/v) low melt agarose-TAE gel prestained with SYBR Safe DNA Gel Stain and resolved for 30 minutes at 120V in 1X TAE running buffer. Alternatively, the low melt agarose-TAE gel can be stained post electrophoresis with BioShop Safe-T-stain for nucleic acid gel stain. Safe-T-Stain (10 µL) was added to 100 mL 1X TAE buffer, the gel was placed in this mixture and was agitated on a table-top shaker for 30 minutes. If the staining was too saturated, the gel was destained in 1X TAE buffer, with agitation, changing the buffer every 5 minutes for 25 minutes. These were visualized with a Bio-Rad Molecular Imager VersaDoc MP 4000. Endonuclease digest products were excised from the low melt agarose gel using a clean razor blade. The digested plasmids were purified following the Nucleospin[®] Gel and PCR clean-up protocol by MACHEREY-NAGEL. Modifications to the MACHEREY-NAGEL protocol include completing the optional wash at step 3, including a second centrifugation at step 4 and eluting the plasmid DNA with 30 µL warmed (65°C) sterile MilliQ water.

Ligation of the PjMetDH-H6::pET28b(+) and NUS-PjMetDH::pET44a(+) constructs

The corresponding restriction endonuclease cut empty plasmids, and gene insert; pET28b with PjMetDH-H6 and pET44a with NUS-PjMetDH, were ligated in final reaction conditions of: gene (PjMetDH) to empty vector ratio of 3:1, 1X Invitrogen T4 DNA ligase buffer, 0.5 µL Invitrogen T4 DNA ligase in a final volume of 10 µL. Ligations were performed at room temperature (20°C) for 1.5 hours. The ligation products were transformed into *E. coli* DH10β cells as described previously. The PjMetDH-H6::pET28b transformed cells were plated on 50 µg/µL kanamycin agar plates, the NUS-PjMetDH::pET44a transformed cells were plated on 50 µg/µL ampicillin agar plates.

Dephosphorylation of the empty pET44a and pET28b plasmids

The restriction endonuclease cut plasmids had their single-stranded overhangs dephosphorylated. Final reaction conditions included 400 ng of plasmid DNA; pET28b and pET44a, 1X New England BioLabs dephosphorylation buffer, 1 μ L of 1 unit/ μ L Calf Intestinal Alkaline Phosphatase (CIAP) from New England BioLabs diluted to a final volume of 40 μ L with sterile MilliQ water. The reaction solution was incubated at 37°C for 30 minutes then 65°C for 15 minutes. Following this dephosphorylation procedure, the plasmid DNA was purified using the Nucleospin[®] Gel and PCR clean-up protocol by MACHEREY-NAGEL as previously described. The dephosphorylated and purified plasmid DNA was then ligated and transformed into *E. coli* DH10 β cells as previously described, transformants were plated onto 50 μ g/ μ L kanamycin or ampicillin agar plates supplemented with 1% (w/v) glucose.

PCR confirmation of positive colonies

Overnight bacterial colonies of the dephosphorylated vectors ligated with the PjMetDH gene insert were screened via PCR to determine if the gene insert was successful. Chosen positive colonies were inoculated into 40 μ L of 10% (v/v) glycerol, resuspended and kept at 4°C. In a final PCR reaction volume of 20 μ L, the reaction components included; 1X BioBasic *Taq* DNA polymerase reaction buffer, 2 mM MgSO₄, 200 μ M dNTPs, 0.5 μ M forward primer, 0.5 μ M reverse primer, 5 units of BioBasic *Taq* (low fidelity) DNA polymerase (HTD0078), 4 μ L of the glycerol- resuspended colony all adjusted to 20 μ L with sterile MilliQ water. The forward primer was the PjMetDH_{intseqFwd} primer, the reverse primer was the T7 terminator primer. The original PjMetDH::pET42b plasmid DNA (1 ng) was used as a positive control, negative controls include 4 μ L of sterile glycerol (10% v/v) and the empty pET28b and pET44a plasmids (1 ng). The PCR cycling conditions were as follows: 94°C for 5 minutes [94°C for 30 seconds, 54°C for 30 seconds, 72°C for 65 seconds] X35 cycles, followed by 72°C for 10 minutes, held at 4°C until removal. The PCR products were resolved on a 1.2% (w/v) agarose gel pre-stained with SYBR Safe DNA Gel stain for 30 minutes at 100V. Positive colonies are expected to have a 1000 bp amplicon.

PjMetDH_{intseqFwd} primer: 5'-CGAAATCATCCTGCGTCAGAC-3'

T7 terminator primer: 5'-GCTAGTTATTGCTCAGCGG-3'

Heat Shock Transformation protocol

Other transformation methods attempted throughout the course of this research included heat shock transformations. Competent *E. coli* DH5 β cells were thawed, plasmid DNA containing the gene insert was added to the competent cell solution (5 μ L DNA solution per 50 μ L cells). This DNA and *E. coli* solution was left on ice for 20 minutes and was then placed in a 42°C bath for 45 seconds, then placed on ice for 5 minutes. These heat shocked cells were then suspended in 500 μ L SOC supplemented with 1% (w/v) glucose and 20 mM MgSO₄, without antibiotics and incubated at 37°C for 1 hour with shaking at 200 rpm. After the 1 hour incubation, cells were centrifuged at 6000 X g for 5 minutes, resuspended in 100 μ L SOC + 1% glucose and plated on the LB agar + 1% (w/v) glucose and their corresponding antibiotic (ampicillin or kanamycin) plates. Plates were incubated overnight at 37°C.

Purification, quantification and restriction endonuclease digest of PjMEtDH-H₆::pET28b Plasmid DNA

Overnight cultures of 6 colonies from the heat shock transformed PjMEtDH-H₆::pET28b cells were chosen for further analysis. Overnight culture final conditions consisted of 1% (w/v) glucose, 50 μ g/mL kanamycin in a total volume of 5 mL LB. These were left to incubate overnight at 37°C with shaking at 250 rpm. Following the incubation period, the plasmid DNA was extracted and purified adhering to the Monarch[®] Plasmid Miniprep Kit by New England BioLabs protocol. Modifications to this protocol include the addition of a second wash buffer 2 wash and the elution of the plasmid DNA with 50 μ L warmed (50°C) sterile MilliQ water. Plasmid DNA was quantified using the NanoDrop 1000 spectrophotometer by Thermo Scientific. This purified PjMEtDH-H₆::pET28b plasmid DNA was digested by the restriction endonuclease pair *Nco*I-HF/*Sa*I-HF in a final reaction condition of 1X NEB Cutsmart buffer, 1.3 μ L of each restriction endonuclease, 1 μ g plasmid DNA adjusted to a final volume of 30 μ L with sterile MilliQ water. The digest was performed at 37°C for 1 hour. The same restriction endonuclease digest was applied to 0.5 μ g of the empty pET28b plasmid. Digested and non-digested products of the plasmid DNA from colonies 1-6 and pET28b empty vector were resolved on a 1.2% (w/v) agarose-TAE gel for 35 minutes at 100V. The gel was stained post electrophoresis with BioShop Safe-T-Stain.

***EcoRI*-HF digest confirmation of PjMetDH-H₆ insert into pET28b**

To further confirm that the PjMetDH-H₆ gene insert was successfully inserted into the pET28b plasmid, the PjMetDH-H₆::pET28b construct as well as the empty pET28b vector was digested with the restriction endonuclease *EcoRI*-HF. Reaction conditions were as follows: 1X NEB CutSmart reaction buffer, 1.3 µL *EcoRI*-HF, 1 µg plasmid DNA, the reaction was adjusted to a final volume of 30 µL with sterile MilliQ water. The digest was completed at 37°C for 1 hour. The digested and non-digested products were resolved on a 1.2 % (w/v) agarose gel run at 100V for 30 minutes. The gel was stained post electrophoresis with BioShop Safe-T-Stain. These procedures were completed twice, the second time the 1.2% (w/v) agarose gel was the pre-staining with SYBR Safe DNA gel stain.

PCR analysis of PjMetDH-H₆::pET28b construct

Colonies 4 and 6 which were believed to have the proper PjMetDH-H₆::pET28b construct were analyzed via PCR. To confirm the proper construct was present in colonies 4 and 6, a PCR with the following reaction conditions was performed on colonies 1-6: 1X *Taq* DNA polymerase reaction buffer, 2 mM MgSO₄, 200 µM dNTPs, 0.5 µM forward primer PjMetDH_{intseqFwd}, 0.5 µM reverse primer T7 terminator primer, 5 units of *Taq* DNA polymerase, 1 ng plasmid DNA, adjusted to a final volume of 20 µL. The empty pET28b vector and water were used as negative controls, the original PjMetDH::pET42b was used as a positive control. The PCR cycling conditions were as followed: 94°C for 5 minutes [94°C for 30 seconds, 54°C for 30 seconds, 72°C for 65 seconds] X35 cycles, followed by 72°C for 10 minutes, held at 4°C. The products were resolved on a 1.2 % (w/v) agarose gel pre-stained with SYBR Safe DNA gel stain for 1 hour at 100V. This procedure was repeated a second time, modifications include changing the annealing temperature from 54°C for 30 seconds to 57°C for 30 seconds, using a different empty pET28b stock, running the products on a 0.8% (w/v) agarose gel and loading the water negative control between the positive PjMetDH::pET42b positive control and the empty pET28b negative control to avoid spilling of the positive control into the negative control wells.

Overnight cultures were made for 6 of the positive PjMetDH-H₆::pET28b clones. Each colony had its plasmid DNA extracted and purified via the Monarch® Plasmid Miniprep Kit by New England BioLabs protocol and quantified using the NanoDrop. Plasmid DNA from the 6 colonies underwent 2 sets of restriction endonuclease digestion one by *Nco*I-HF/*Sal*-HF and one by *Eco*RI-HF with reaction conditions described previously. Restriction endonuclease digest products were resolved on a 0.8 % (w/v) agarose gel prestained with SYBR Safe DNA Gel stain at 100V for 35 minutes. Following the results of this gel, colonies 1 and 3 were sent for Sanger sequencing at Genome Quebec. The sequencing primers used were the PjMetDH_{intseq}Fwd primer and the T7 terminator primer.

Protein Expression trial 1

Electrotransformation of PjMetDH::pET42b and pGEX-4T-3 into E. coli RIPL cells

PjMetDH::pET42b and pGEX-4T-3 plasmid DNA (100 ng) were transformed into electrocompetent *E. coli* BL21 CodonPlus (DE3) RIPL cells. Time constants were 5.6 and 5.5 ms respectively. Cells were recovered in 500 µL LB media and incubated at 37°C for 45 minutes with agitation at 200 rpm. Cells were plated onto ampicillin + 1% (w/v) glucose or kanamycin plates and incubated overnight at 37°C. Overnight cultures were made for 6 of the positive PjMetDH::pET42b clones.

Day cultures of E. coli RIPL transfected with PjMetDH::pET42b

Day cultures of *E. coli* RIPL cells transfected with PjMetDH::pET42b were prepared firstly by measuring cell growth using the Molecular Devices M3 microplate spectrophotometer Softmax Pro program to measure optical density (OD) at 600 nm. Measurements were taken of 1:5; 1:10, and 1:20 dilutions of the overnight cultures. The volume of overnight cell culture needed in a final day culture volume of 400 mL LB-phosphate buffer (0.1 M sodium phosphate, pH 7.8 (Prasad *et al.*, 2011)) to obtain a starting OD of 0.05, was calculated. There was an insufficient amount of overnight cultures to attain the desired 0.05OD starting point, therefore what was available was added to the day culture and the day culture started below 0.05 OD at 0.019OD. Day cultures also contained 50 µg/mL kanamycin. Day cultures were incubated at 37°C at 200 rpm, the optical density was measured every hour until it was between 0.6-0.8 OD. Once the optical density was between 0.6-0.8 the day culture was placed on ice for 10 minutes,

then protein expression was induced with isopropyl β -D-1-thiogalactopyranoside (IPTG) at a final concentration of 500 μ M. The day cultures were incubated at 20°C at 250 rpm for 3 hours.

Harvesting and homogenization of E. coli RIPL cells

Following the induction of protein expression, cells were harvested. The day culture was centrifuged at 10000 X g at 4°C for 10 minutes. The supernatant was discarded, and the cell pellet was resuspended in equal volume (400 mL) 10 % (v/v) glycerol. Resuspended cells were then centrifuged at 10000 X g at 4°C for 10 minutes. The supernatant was discarded, and the pellet was resuspended in 10 mL 1X phosphate-buffered saline (PBS: 137 mM NaCl, 2.7 mM KCl, 10 mM Na₂HPO₄, 1.8 mM KH₂PO₄). This was frozen in liquid nitrogen and stored at -80°C until homogenization. Cells were lysed by passing them through the Avestin Emulsiflex B-15 homogenizer 3 times at 21 000 psi. The produced lysate was centrifuged at 12000 X g at 2°C for 20 minutes. The supernatant and the pellet were separated, and the protein content of each was determined as follows. The pellet or the insoluble fraction was solubilized by adding 200 μ L of 4X Laemmli sample buffer (LBS), boiling it for 5 minutes at 100°C, and then centrifuging for 2 minutes at 10000 X g; this was called the solubilized-insoluble fraction. Protein concentration from the insoluble fraction was qualitatively determined by blotting the solubilized-insoluble fraction on a blotting paper as well as bovine serum albumin (BSA) protein standards of 0.05, 0.1, 0.2, 0.3, 0.4, 0.5, 1.0, 2.0, 2.5, 5.0, 7.5, and 10.0 mg/mL. The soluble fraction protein concentration was quantified by the Bradford assay method (Bradford, 1976). The soluble and insoluble fractions were compared via SDS-PAGE gel analysis.

Protein purification

An Econo-Pac[®] (BioRad) column was washed, cleaned, and a 1 mL gel bed of the glutathione sepharose 4 fast flow resin (GE Healthcare Life Sciences) was poured. This was treated with 10 mL 1X PBS with 320 mM 2-mercaptoethanol to reduce the glutathione. The column was then equilibrated with 10 mL 1X PBS. The protein solution was then loaded onto the column and the non-binding eluate (NBE) collected. The column was washed with 10 mL 1X PBS with 5 mM dithiothreitol (DTT) and collected as the 'Wash' fraction. Proteins were eluted from the resin in 1 mL fractions for a total of 10 fractions with 50 mM Tris-HCl (pH 8.0) 10 mM reduced glutathione. Protein concentration for all fractions was determined using the Bradford assay method (Bradford, 1976). SDS-PAGE analysis was performed for each fraction.

Desalting of purified GST-PjMetDH

The elution fractions that were determined to have protein were pooled and centrifuged at 5000 X g, 4°C, for 15 minutes in an Amicon[®] Ultra-15 centrifugal concentrator (10 000 MWCO). The pooled elution fraction volume was 4 mL, therefore after each centrifugation the volume was brought back up to this original volume with 1X PBS until the final centrifugation where this was not repeated. A total of 3 centrifugations were completed. To maximize protein recovery, the membrane surfaces were washed with a minimal volume of 1X PBS and added to the recovered and concentrated fraction. Protein concentration of the concentrated solution was determined by Bradford assay (Bradford, 1976).

Thrombin cleavage

The purified and desalted GST-PjMetDH (8.82 µg) was digested with thrombin at a ratio of 30 units thrombin/mg GST-PjMetDH. The digest was completed at 25°C. Samples were taken from this reaction for SDS-PAGE analysis at 0, 1, 2, 4, 6 and 24 hours. The optimal incubation time was determined to be 2 hours.

Kinetic assay of the impure, cleaved GST PjMetDH

A primary activity assay was conducted on the impure, cleaved GST-PjMetDH solution. Final reaction conditions are as followed: 100 mM glycine-KOH (pH 10.5), 100 mM KCl, 2.5 mM NAD⁺ or NADP⁺, 10 mM amino acid and 156 ng impure, cleaved GST PjMetDH protein solution. The amino acids evaluated in triplicate were glutamic acid, leucine, valine, phenylalanine, and methionine. Absorbance was measured at 340 nm with measurements every 16 seconds for 10 minutes. As there was no noticeable activity in this initial assay, a further assay was conducted, utilizing lower protein concentrations including 0, 3.13, 6.25, 12.5, 37.5, 75 and 150 ng being assayed with both NAD⁺ and NADP⁺ and only against the amino acid methionine.

Purification of PjMetDH from GST

In an Econo-Pac[®] column, a 1mL gel bed of the glutathione sepharose 4 fast flow resin solution by GE Healthcare Life Sciences was poured. The column was washed with 10 mL 1X PBS with 320 mM 2-mercaptoethanol. The cleaved GST PjMetDH solution was loaded onto the column and the NBE containing the PjMetDH was collected. The column was then washed

with 8 mL of 1X PBS. GST or uncleaved GST-PjMetDH protein was eluted with 5 mL 50 mM Tris-HCl (pH 8.0).

Desalting of cleaved PjMetDH

The flow through containing the cleaved PjMetDH was quantified by Bradford assay and analysed by SDS-PAGE gel.

Protein expression trial 2

With the goal of increasing the GST-PjMetDH protein yield in each bacterial culture, a second protein expression trial was conducted. The electrotransformation and day culture procedures remained the same. Protein expression induction was allowed to proceed for approximately 16 hours (overnight) rather than 3 hours. Cells were harvested and homogenized as previously described. The protein purification steps remain unchanged.

Thrombin cleavage

The purified but not desalted GST-PjMetDH solution was digested with thrombin at a ratio of 30 units thrombin/mg GST-PjMetDH. In this trial, the protein sample was not desalted, therefore the digest reaction was supplemented with 150 mM NaCl, 2.5 mM CaCl₂ and 0.1% (v/v) 2-mercaptoethanol to yield maximum thrombin activity.

Desalting of purified, cleaved PjMetDH: Nanosep concentrator

The first attempt at desalting the purified GST-PjMetDH protein was completed using a Nanosep[®] Centrifugal Device with 10K Omega Membrane. The protein solution (2X 500 µL) was centrifuged at 14 000 X g for 25 minutes at 4°C. PBS (1X) was added to the concentrator to the original volume after each centrifugation. The following 5 centrifugations were adjusted to 10 minutes.

Desalting of purified, cleaved PjMetDH: desalting column

The purified, cleaved PjMetDH protein sample was desalted using an Econo-Pac[®] 10DG desalting column (BioRad, Cat. No. 732-2010) as per manufacturers instructions. The column was equilibrated with two column volumes (20 mL) 1X PBS, the protein sample was then loaded onto the column, then 4 mL of 1X PBS was added, and the flow through was collected in 1mL fractions. Sub-samples were saved for protein quantification and SDS-PAGE analysis.

Desalting of purified, cleaved PjMetDH: dialysis cassette

The protein recovered from the desalting column frit was adjusted to a total volume of 12 mL and loaded into a PIERCE Slide-A-Lyzer[®] dialysis cassette, 7 000 MWCO (No. 66710, 3-12 mL sample volume) as directed by the product manual. The dialysis cassette was placed in 1L of 1X PBS, at 4°C with stirring. Buffer exchanges were completed at 3, 6, 9, and 16 hours. This desalted, purified, and cleaved PjMetDH solution was further purified of GST or GST-PjMetDH using the glutathione affinity column as previously described.

Glutathione colorimetric assay

The effectiveness of the dialysis cassette to successfully remove the free reduced glutathione was determined by a glutathione assay. Ellman's reagent (or, 5,5'-dithiobis-(2-nitrobenzoic acid, DTNB) was made up in dimethyl sulfoxide (DMSO) to 10 mM, and diluted 100-fold with 0.1 M Tris-HCl (pH 7.5). Samples were treated with this, incubated for 2 minutes then absorbance was measured at 412 nm. The molar extinction coefficient of Ellman's reagent is $14.15 \text{ M}^{-1}\text{cm}^{-1}$ (Eyer *et al.*, 2003).

Results

Phylogenetic relationship of PjMetDH and other amino acid dehydrogenases

The evidence presented to validate the belonging of the putative *Polysiphonia* methionine dehydrogenase to the Glu/Leu/Phe/Val (ELFV) dehydrogenase family include a neighbour-joining phylogenetic tree analysis comparing PjMetDH to other amino acid dehydrogenases as well as a multiple protein sequence alignment comparing PjMetDH to known members of the Glu/Leu/Phe/Val dehydrogenase family. Firstly, the phylogenetic relationship of the protein sequence of the PjMetDH protein was compared to other known amino acid dehydrogenases (figure 6). This neighbour-joining phylogenetic tree places the *Polysiphonia* methionine dehydrogenase as being closely related to those of the Glu/Leu/Phe/Val dehydrogenase family rather than other amino acid dehydrogenases.

To further validate the belonging of PjMetDH in the Glu/Leu/Phe/Val dehydrogenase family, a multiple protein sequence alignment comparing PjMetDH to two phenylalanine dehydrogenases, an alanine dehydrogenase, leucine dehydrogenase and a valine dehydrogenase was prepared. Many critical catalytic residues found in most amino acid dehydrogenases, including Lys68(Δ), Lys80(\blacklozenge) were conserved in the methionine dehydrogenase at study (figure 7). Amino acid residues that have been found to be involved in cofactor binding or shaping the cofactor binding pocket include; Gly77(\circ), Gly78(\bullet), Ser147(β), Gln179(\P), Gly180(ϕ), Val204(\times), Isoleucine204 (\sim), Ala238 (\S), Leu239 (\emptyset), Ser259 (\div), Asn261 (δ) and Gly290 (θ) (Baker *et al.*, 1995; Sekimoto *et al.*, 1994; Yamaguchi *et al.*, 2019). Other important amino acid residues investigated include those that have been found to be important to substrate specificity, specifically involved in shifting activity towards *L*-methionine, these include Gly124 (α) and Leu304 (λ) (Seah *et al.*, 1995, 2003). Other amino acids denoted as \blacktriangle , \pounds , \pm and \copyright have also been found to be important in catalysis by (Chen and Engel, 2009)

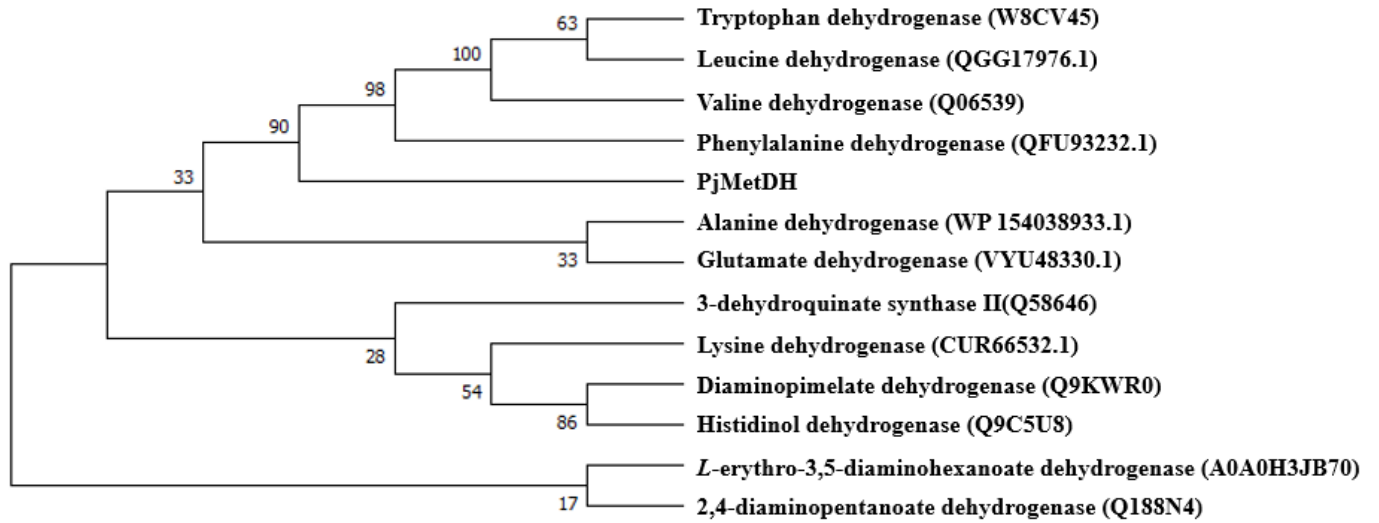


Figure 6: Neighbour-joining phylogenetic tree of PjMetDH and other amino acid dehydrogenase enzymes. The protein sequences were retrieved from NCBI and the accession numbers are given in brackets next to the enzyme name. Phylogeny was determined using 1000 bootstrap replications, evolutionary distances were determined using the “number of differences method”. The phylogenetic tree was generated using the MEGA7 software.

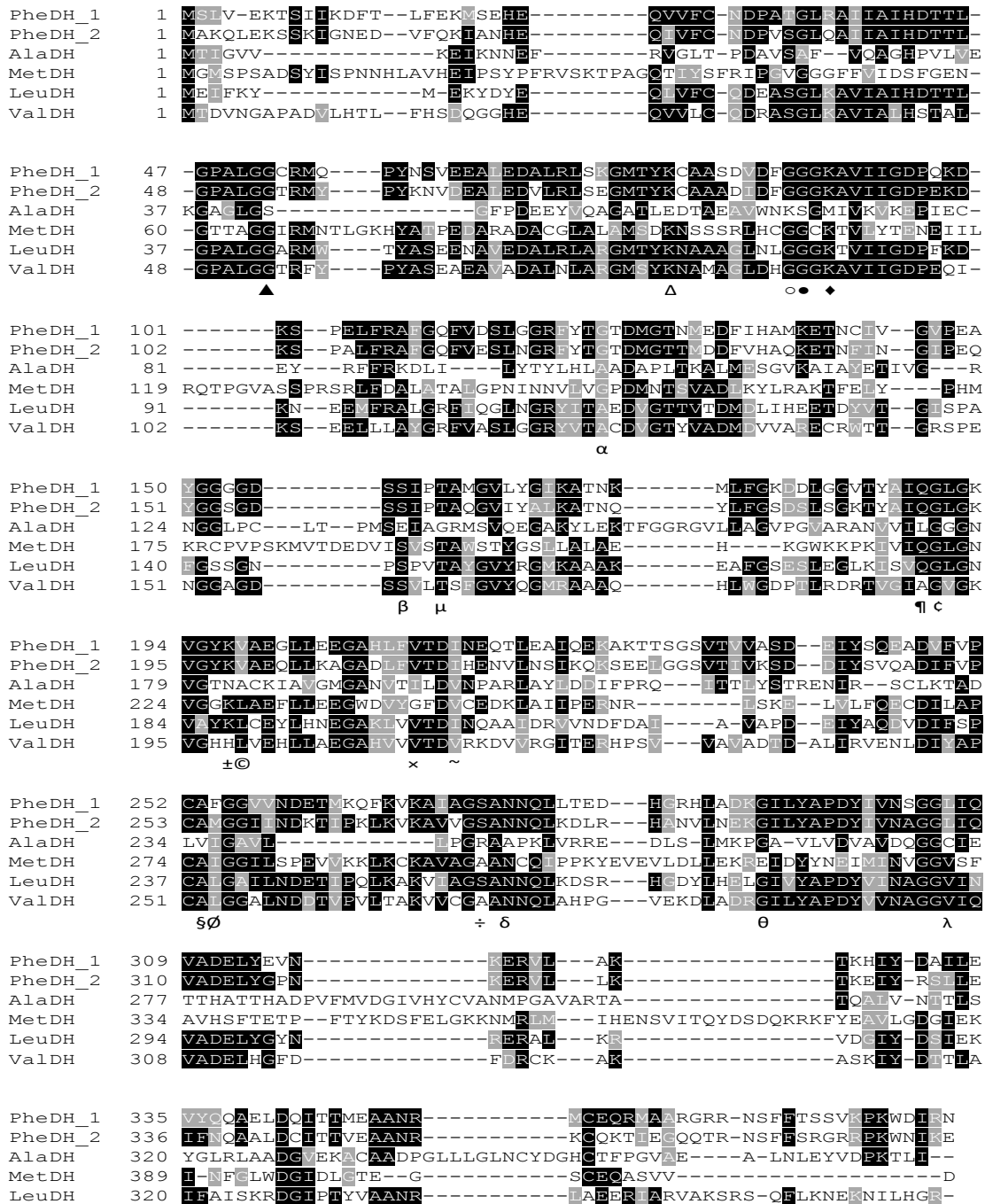


Figure 7: Multiple sequence alignment of PjMetDH protein sequence compared to other amino acid dehydrogenases from the Glu/Leu/Phe/Val dehydrogenase family. Amino acid dehydrogenases include two phenylalanine dehydrogenases, one alanine dehydrogenase and one leucine dehydrogenase. The sequence alignment was completed using the T-Coffee multiple sequence alignment server and coloured with the BoxShade software. PheDH_1: phenylalanine dehydrogenase from *Bacillus badius* (BAA08816.1). PheDH_2: phenylalanine dehydrogenase from *Lysinibacillus sphaericus* (AAA22646.1). AlaDH: alanine dehydrogenase from *Clostridiales bacterium* (WP_154038933.1). LeuDH: leucine dehydrogenase from *L. sphaericus* (KEK12366.1).

Cloning of PjMetDH constructs

To maximize the chances of success in heterologously expressing and purifying the recombinant PjMetDH protein, we aimed to produce three constructs. The first would have a GST affinity tag fused to the N-terminus of the PjMetDH protein, denoted GST-PjMetDH::pET42b, the second; an N-terminal hexahistidine (H₆)-NUS solubility tag denoted NUS-PjMetDH::pET44a, and the third; a C-terminal H₆ tag, denoted PjMetDH-H₆::pET28b. Stock solutions of the empty pET44a and pET28b vectors were digested with the appropriate restriction endonucleases required to produce either the H₆ or NUS tags (figure 8). Similarly, the originally supplied GST-PjMetDH::pET42b construct was digested by the same sets of restriction endonucleases to create gene inserts for the ligation reaction. The products of these restriction endonuclease digests can be seen in figure 8. Figure 8 should not be used to measure DNA product size as this gel electrophoresis served only to separate the digested PjMetDH gene insert from its original plasmid, DNA products did not resolve for a sufficient amount of time to infer product size. In figure 9 however, there is the Nucleospin gel- and PCR-purified DNA products from figure 8, resolved completely for DNA fragment size determination. The PjMetDH gene insert appears at approximately their expected bp length of 1253 bp, the digested pET28b vector appears near its empty vector length of 5.4 kb, as well as the pET44a empty vector appearing at its known length of 7.3 kb.

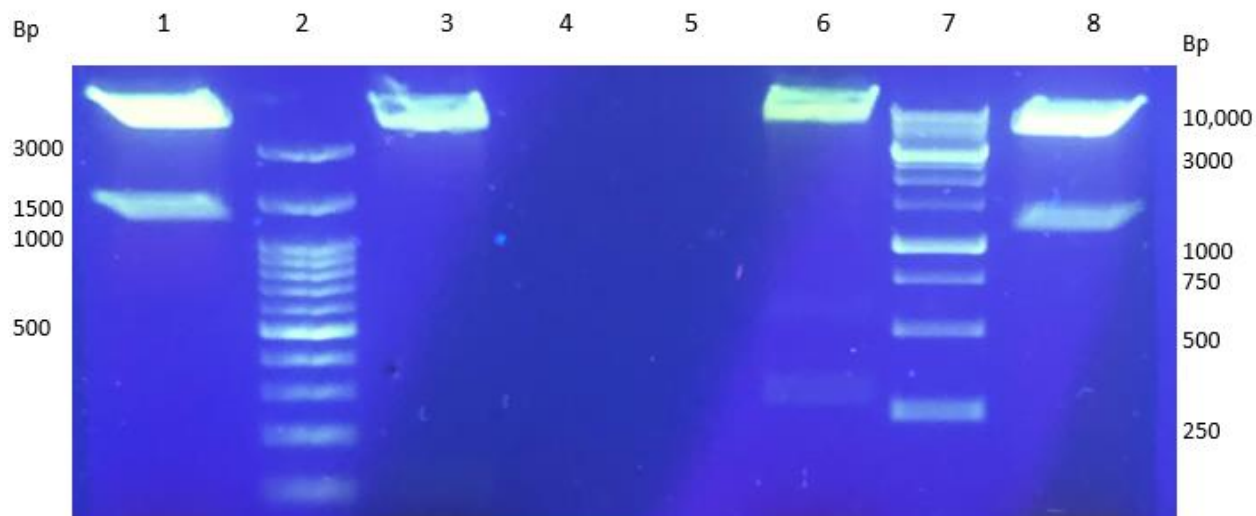


Figure 8: Low melt agarose (1.2% (w/v) in TAE) electrophoresis analysis of the restriction endonuclease digest of the pET44a and pET28b vectors and the GST-PjMetDH::pET42b constructs. Lane 1: PjMetDH::pET42b digested by *SpeI/XhoI*; Lane 2: 100 bp DNA ladder (GeneDirex); Lane 3: pET28b vector digested by *NcoI/SalI*; Lanes 4 and 5: empty; Lane 6: pET44a digested by *SpeI/XhoI*; Lane 7: 1 kb ladder (GeneDirex); Lane 9: PjMetDH::pET42b digested by *NcoI/SalI*.

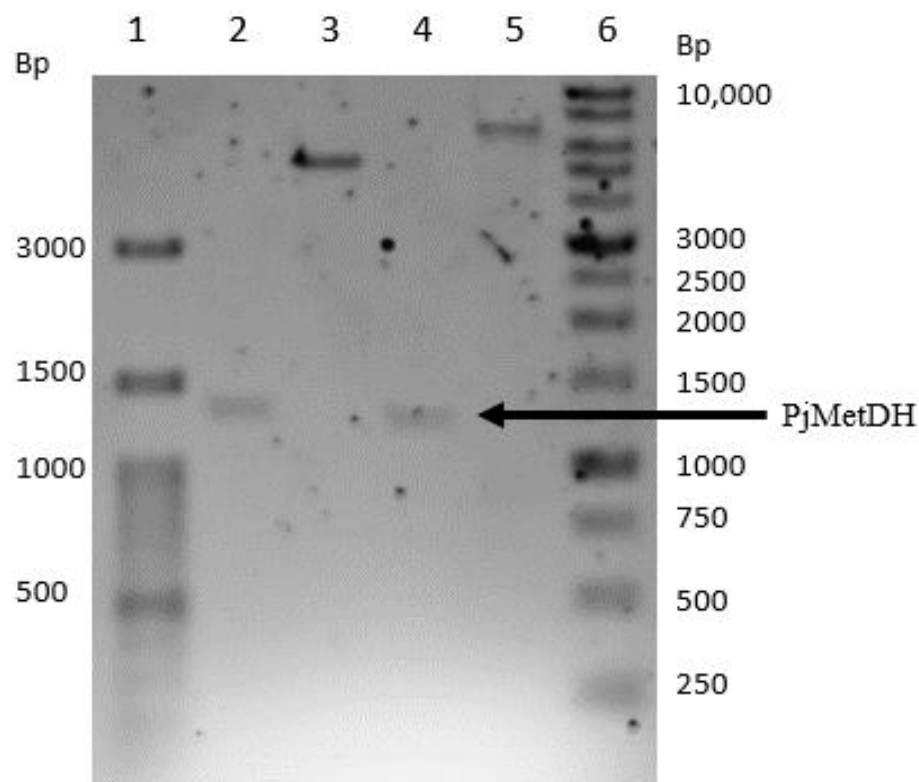


Figure 9: Agarose (1.2% (w/v) in TAE) gel electrophoresis analysis of purified DNA products. DNA products were purified via the Nucleospin Gel and PCR cleanup protocol, here the purified products are confirmed. Lane 1: 100 bp DNA ladder (GeneDirex); Lane 2: *XhoI/SpeI* digested PjMetDH::pET42b; Lane 3: *NcoI/SalI* digested pET28b; Lane 4: *NcoI/SalI* digested PjMetDH::pET42b; Lane 5: *SpeI/XhoI* digested pET44a; Lane 6: 1 kb ladder (GeneDirex).

Once positive clones, containing the properly ligated and transformed NUS-PjMetDH::pET44a, and PjMetDH-H₆::pET28b constructs were identified via antibiotic resistance testing, plasmid DNA was extracted from multiple colonies and assessed via PCR. An internal primer specific to the PjMetDH gene insert, as well as a commonly used reverse primer were employed to amplify a section of the two constructs that had an expected length of approximately 1000bp. In figure 10, agarose gel electrophoresis analysis of the PCR products for what were considered to be 19 positive clones containing the NUS-PjMetDH::pET44a construct are shown. A 1000 bp DNA fragment was not observed in any of the PCR reactions on what were thought to be positive clones. Lanes 1-19 contain the sampled colonies, and lane 21 contains the positive control: the original GST-PjMetDH::pET42b. Comparing the two it is clear that these clones do not possess the proper gene insert. At this point it was thought that

self-ligation had caused the results seen in figure 10, therefore other methods, such as dephosphorylating the digested vectors prior to the ligation reaction, as well as heat shock transformations were explored. The heat shock transformation technique yielded fewer successful clones compared to electrotransformations, and it was determined that dephosphorylating the digested and empty vectors was favourable.

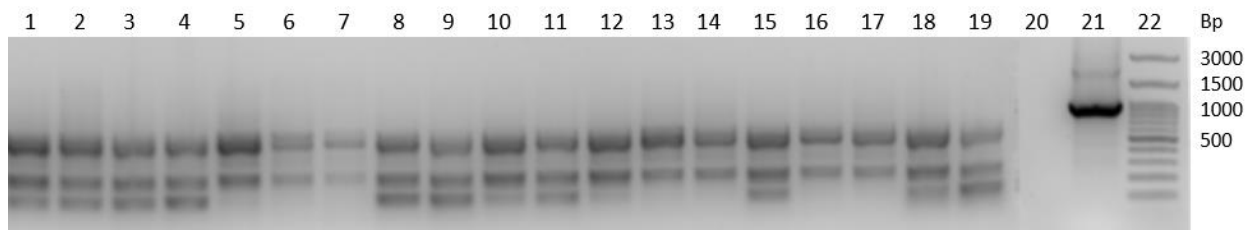


Figure 10: Agarose (1.2% (w/v) in TAE) gel electrophoresis analysis of the PCR products for the detection of positive clones. Positive clones defined as having the PjMetDH DNA sequence properly inserted into the empty pET44a vector. Designed primers for detection of proper PjMetDH gene insert should yield an expected PCR amplicon length of 1000 bp. Lanes 1-19: colony picks 1-18; Lane 19: empty pET44a vector (negative control); Lane 20: water (negative control); Lane 21: PjMetDH::pET42b (positive control); Lane 22: 100 bp ladder (GeneDirex).

The PjMetDH-H₆::pET28b construct was produced having dephosphorylated the digested empty pET28b vector. An important feature of the PjMetDH-H₆::pET28b construct is that, when properly assembled, this construct has a single cleavage site for the restriction endonuclease *EcoRI*, which is found in the PjMetDH gene insert portion. This feature allows us to screen possible positive clones by harvesting and digesting clone plasmid DNA with *EcoRI*, this action should result in the DNA construct linearizing, allowing us to more effectively screen for DNA constructs of the expected size, in the case of the PjMetDH-H₆::pET28b construct, the expected size is approximately 7 kb. In figure 11, we have the products of the digestion of plasmid DNA from 6 potentially positive clones with the restriction endonuclease *EcoRI*. The results from this experiment were inconclusive as both the digested and undigested samples resolved at similar lengths, as well as the 1 kb ladder being degraded, however clones from colonies 4 and 6 seemed promising as their DNA bands resolved closer to what was expected to be 7 kb.

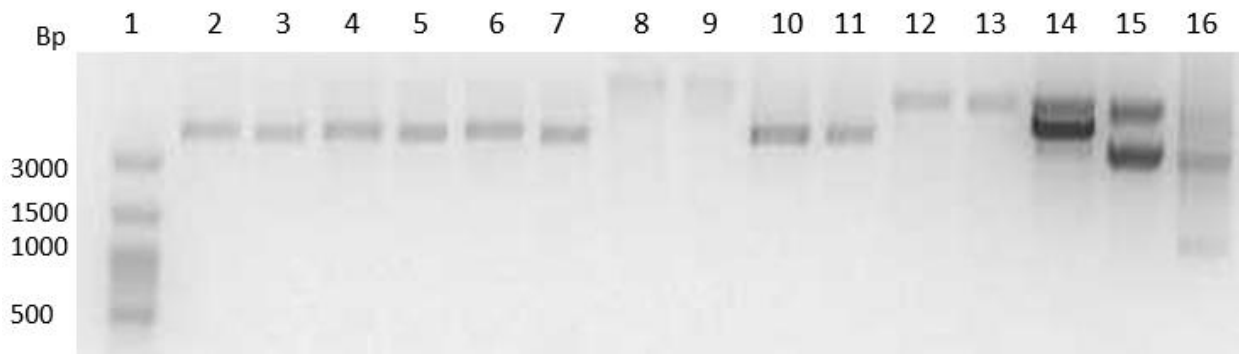


Figure 11: Agarose (1.2% (w/v) in TAE) gel electrophoresis analysis of *EcoRI*-digested PjMetDH-H₆::pET28b constructs. Lane 1: 100 bp ladder (GeneDirex); Lane 2: colony pick 1 plasmid DNA digested with *EcoRI*; Lane 3: colony pick 1 plasmid DNA un-digested; Lane 4: colony pick 2 plasmid DNA digested with *EcoRI*; Lane 5: colony pick 2 plasmid DNA un-digested; Lane 6: colony pick 3 plasmid DNA digested with *EcoRI*; Lane 7: colony pick 3 plasmid DNA un-digested; Lane 8: colony pick 4 plasmid DNA digested with *EcoRI*; Lane 9: colony pick 4 plasmid DNA un-digested; Lane 10: colony pick 5 plasmid DNA digested with *EcoRI*; Lane 11: colony pick 5 plasmid DNA un-digested; Lane 12: colony pick 6 plasmid DNA digested with *EcoRI*; Lane 13: colony pick 6 plasmid DNA un-digested; Lane 14: *EcoRI* digested pET28b vector; Lane 15: undigested pET28b vector; Lane 16: 1 kb ladder (GeneDirex).

The same six hypothesized positive clones for the PjMetDH-H₆::pET28b construct used in the endonuclease digest of figure 11 were also analyzed by the previously mentioned PCR method to validate positive clones. In the case of these 6 clones, figure 12 shows the agarose gel electrophoresis of the PCR reactions, an amplicon of the expected 1000 bp size was observed in all clones, however it was also found in the empty pET28b vector negative control, suggesting contamination had occurred. This PCR analysis was conducted a second time on these same 6 clones, and the aliquot of empty pET28b vector that was used as a negative control was changed, the results of this are found in figure 13. In this reaction, amplicons of the expected 1000 bp length were found in 3 of the colonies and the positive control but was not found in the empty pET28b vector. The issue that arose in this trial is that three of the colony picks seemed to have no DNA products present, when, in the last trial some contaminating bands were found regardless of proper gene insertion, suggesting that not enough plasmid DNA was added to the PCR reaction. This put the negative result from the empty pET28b vector negative control on uncertain terms. In light of the restriction endonuclease and PCR reaction results, it was believed that the gene insert had been properly ligated into the PjMetDH-H₆::pET28b construct.

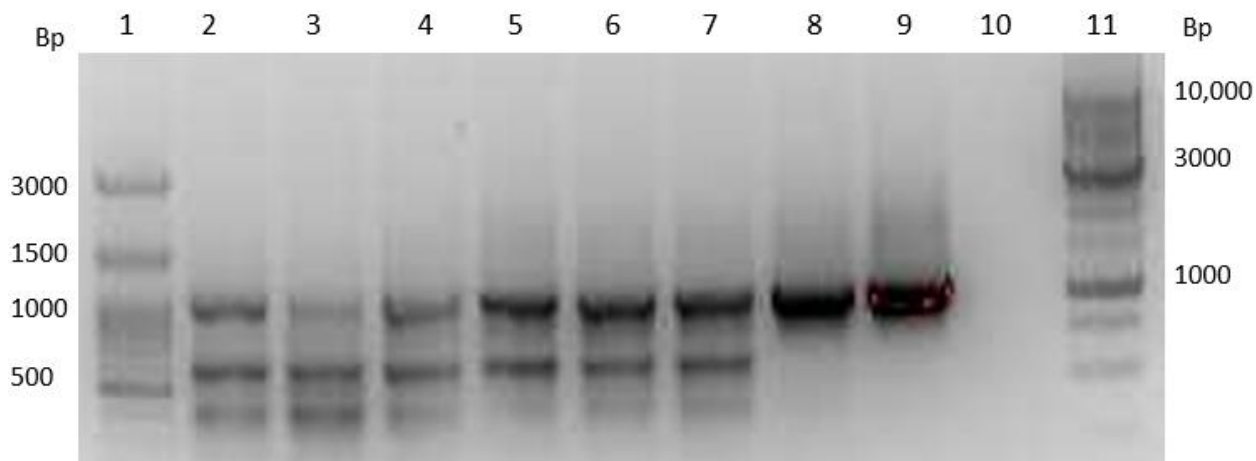


Figure 12: Agarose (1.2% (w/v) in TAE) gel electrophoresis analysis of the PCR products for the detection of positive clones. Positive clones defined as having the PjMetDH DNA sequence properly inserted into the empty pET28b vector. Designed primers for detection of proper PjMetDH gene insert should yield an expected PCR amplicon length of 1000 bp. Lane 1: 100 bp ladder (GeneDirex); Lane 2: colony pick 1 plasmid DNA PCR products; Lane 3: colony 2 PCR products; Lane 4: colony 3 PCR products; Lane 4: colony 4 PCR products; Lane 5: colony 4 PCR products; Lane 6: colony 5 PCR products; Lane 7: colony 6 PCR products; Lane 8: PjMetDH::pET42b construct; Lane 9: pET28b vector (negative control); Lane 10: water (negative control); Lane 11: 1 kb ladder (GeneDirex).

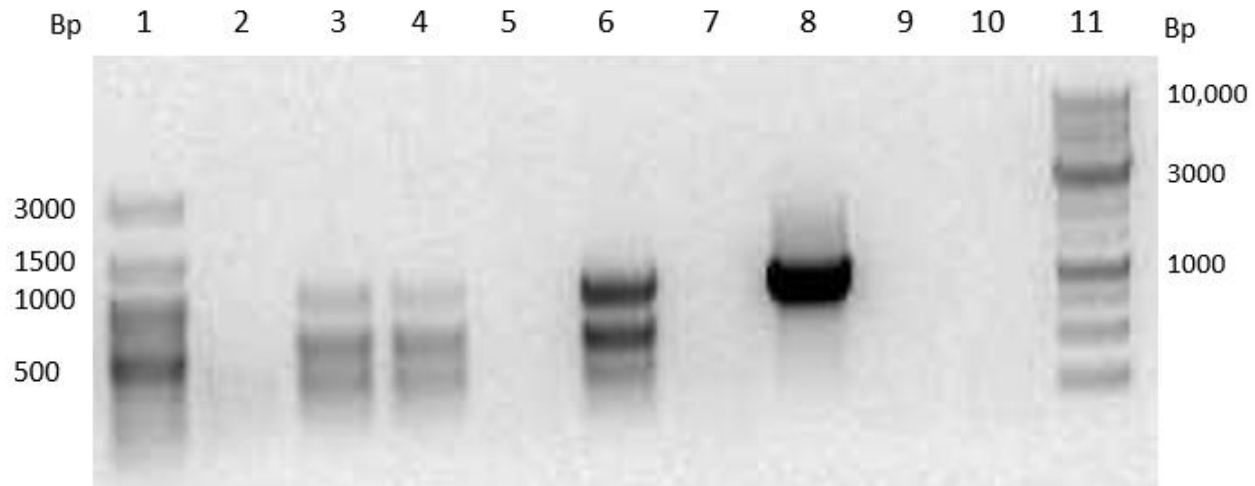


Figure 13: Agarose (0.8% (w/v) in TAE) gel electrophoresis analysis on the PCR products for the detection of positive clones. PCR analysis was conducted a second time on the 6 colony picks following conflicting results of the first PCR analysis. Positive clones defined as having the PjMetDH DNA sequence properly inserted into the empty pET28b vector. Designed primers for detection of proper PjMetDH gene insert should yield an expected PCR amplicon length of 1000 bp. Lane 1: 100 bp ladder (GeneDirex); Lane 2: colony pick 1 plasmid DNA PCR products; Lane 3: colony 2 PCR products; Lane 4: colony 3 PCR products; Lane 5: colony 4 PCR products; Lane 6: colony 5 PCR products; Lane 7: colony 6 PCR products; Lane 8: PjMetDH::pET42b PCR products; Lane 9: water (negative control); Lane 10: pET28b empty vector (negative control); Lane 11: 1 kb ladder (GeneDirex).

One final experiment to confirm the PjMetDH-H₆::pET28b construct was completed, this involved digesting the PjMetDH-H₆::pET28b construct with the restriction endonucleases that had originally been used to digest the empty pET28b vector. This would result in the removal of the gene insert, these were compared to the same construct being digested with *EcoRI* as well as an undigested sample, all of which were visualized on an agarose gel, the results of this experiment are found in figure 14. The constructs which had been digested by the *EcoRI* endonuclease were expected to linearize and appear at approximately 7 kb, where the constructs which were digested with both *NcoI* and *SalI* endonucleases were expected to have two DNA product, one being the gene insert at an expected length of 1200 bp and a second representing the empty vector at approximately 5.4kb. In colonies 1, 2, 3 and 5, the *EcoRI* digested and undigested constructs resolved at a shorter base pair length than expected. However, the *NcoI/SalI* endonuclease digests produced two DNA products, both at approximately the expected sizes. In the case of clones from colonies 4 and 6, we did observe

results that were inconsistent with what was expected. The *EcoRI* digested and the undigested samples for both colonies resolved at a much higher base pair length than expected, near 9000 bp, however the results from the *NcoI/SalI* digest were consistent with the expected results, that is one band just over 1000 bp and a second at about 7 kb. With these conflicting results, the decision was made to send colonies 1 and 3 for sequencing at Genome Quebec. The results from Genome Quebec indicated the gene insert as the *U. mutabilis* MTOB reductase gene.

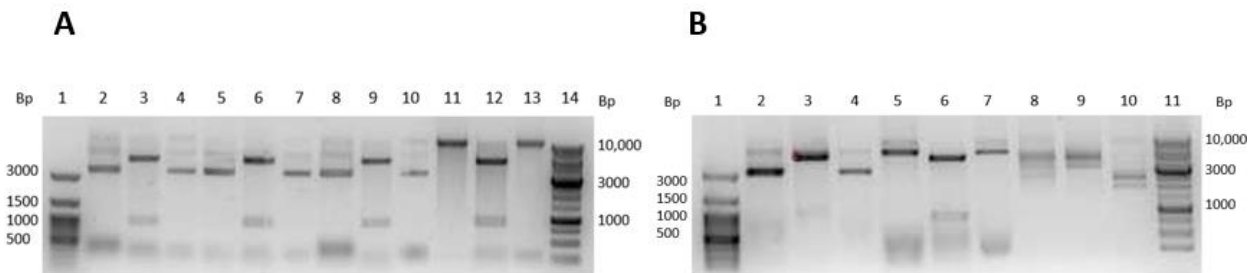


Figure 14: Agarose (0.8% (w/v) in TAE) gel electrophoresis analysis of restriction endonuclease digested PjMetDH-H₆::pET28b construct colonies. **A)** Restriction endonuclease digest of colonies 1 through 4. Lane 1: 100 bp ladder (GeneDirex); Lane 2: *EcoRI* digest of colony 1 plasmid DNA; Lane 3: *NcoI/SalI* digest of colony 1 plasmid DNA; Lane 4: undigested colony 1 plasmid DNA; Lane 5: *EcoRI* digest of colony 2 plasmid DNA; Lane 6: *NcoI/SalI* digest of colony 2 plasmid DNA; Lane 7: undigested colony 2 plasmid DNA; Lane 8: *EcoRI* digest of colony 3 plasmid DNA; Lane 9: *NcoI/SalI* digest of colony 3 plasmid DNA; Lane 10: undigested colony 3 plasmid DNA; Lane 11: *EcoRI* digest of colony 4 plasmid DNA; Lane 12: *NcoI/SalI* digest of colony 4 plasmid DNA; Lane 13: undigested colony 4 plasmid DNA; Lane 14: 1 kb ladder (GeneDirex). **B)** Restriction endonuclease digest of colonies 5 and 6. Lane 1: 100 bp ladder (GeneDirex); Lane 2: *EcoRI* digest of colony 5 plasmid DNA; Lane 3: *NcoI/SalI* digest of colony 5 plasmid DNA; Lane 4: undigested colony 5 plasmid DNA; Lane 5: *EcoRI* digest of colony 6 plasmid DNA; Lane 6: *NcoI/SalI* digest of colony 6 plasmid DNA; Lane 7: undigested colony 6 plasmid DNA; Lane 8: *EcoRI* digested pET28b empty vector; Lane 9: *NcoI/SalI* digested pET28b empty vector; Lane 10: undigested pET28b empty vector; Lane 11: 1 kb ladder (GeneDirex).

Protein expression trial 1

Protein expression trials were performed with the GST-PjMetDH::pET42b construct as we were unable to create the other two PjMetDH expression plasmids. Successful protein expression would result in a 71 kDa GST-PjMetDH protein. Protein expression was compared in all stages of purification, beginning with the insoluble and soluble fractions of the first stage of purification. In figure 15 we compared the proteins found in the soluble and insoluble fractions at increasing concentration at 10, 20 and 30 μg . The insoluble protein samples were overloaded; therefore, we cannot properly compare the soluble and insoluble fractions, however in the soluble fractions we can clearly observe a protein band at approximately the expected 71 kDa size. The overloading of the insoluble fractions was likely due to the inaccurate under-estimation of protein concentration via dot blot analysis (not shown here).

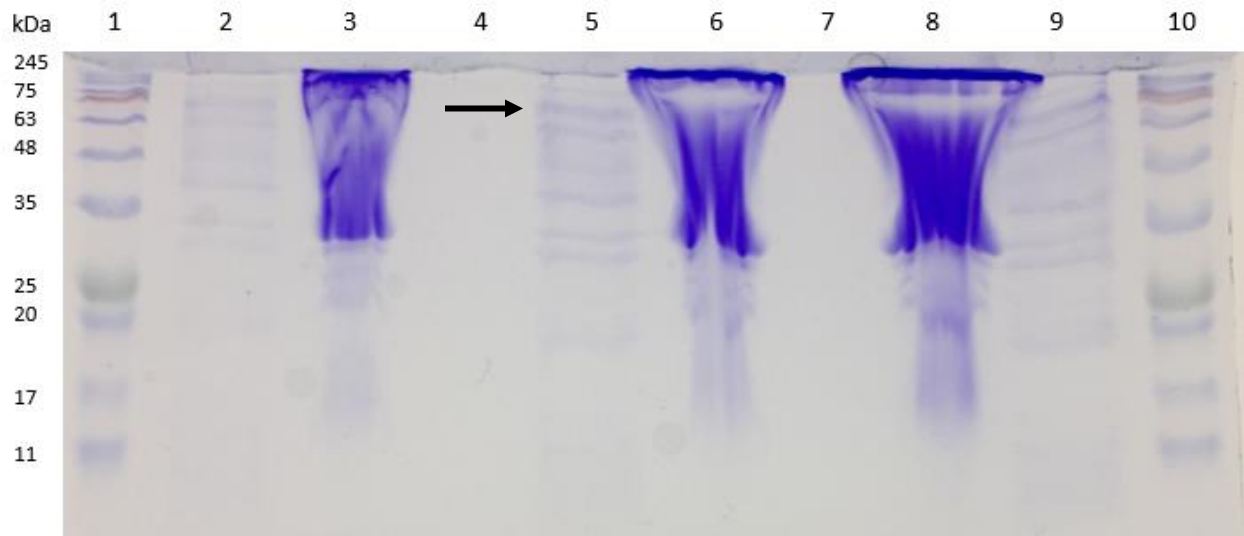


Figure 15: SDS-PAGE (10% (w/v)) gel comparison of the soluble and insoluble fractions of the homogenized bacterial overexpression cells. GST-PjMetDH::pET42b/RIPL cells were grown in LB-phosphate with 50 $\mu\text{g}/\text{mL}$ kanamycin, 200 rpm, at 37°C. Protein expression was induced in cells with 500 μM IPTG for 3 hours. Cells were lysed by passing the cell suspension through the Avestin Emulsiflex homogenizer three times at 21000 psi. The lysate was centrifuged at 12000 X g for 20 minutes at 2°C, the pellet was denoted as the insoluble fraction and the supernatant denoted as the soluble fraction. Lane 1: MBI rainbow protein molecular weight ladder; Lane 2: soluble fraction (~10 μg); Lane 3: insoluble fraction (~10 μg); Lane 4: empty; Lane 5: soluble fraction (~20 μg); Lane 6: insoluble fraction (~20 μg); Lane 7: empty; Lane 8: insoluble fraction (~30 μg); Lane 9: soluble fraction (~30 μg); Lane 10: MBI rainbow protein molecular weight ladder. The GST-PjMetDH is indicated by an arrow. The SDS-PAGE gel was stained in Coomassie Brilliant Blue R-250 overnight with agitation.

Further purification stages involved the use of glutathione-affinity columns where the GST-tagged PjMetDH was selectively purified from other contaminating proteins. In all fractions but the wash fraction visualized in figure 16, a protein of the expected 71 kDa size is observed. Furthermore, contaminating proteins are seen to visually decrease in number with increasing purification steps. In figure 16, all successful purification steps are presented. From left to right samples increase in purity, beginning with the insoluble protein fraction, followed by the soluble fraction, then the non-binding eluate and wash fractions from the GSH affinity column and finally the elution fractions. Throughout these purification steps, the GST-PjMetDH is expected to be found in all fractions to some extent, but less so in the wash fraction. The results from figure 16 confirm that purification was successful as contaminating proteins are less abundant in increasing purification stages.

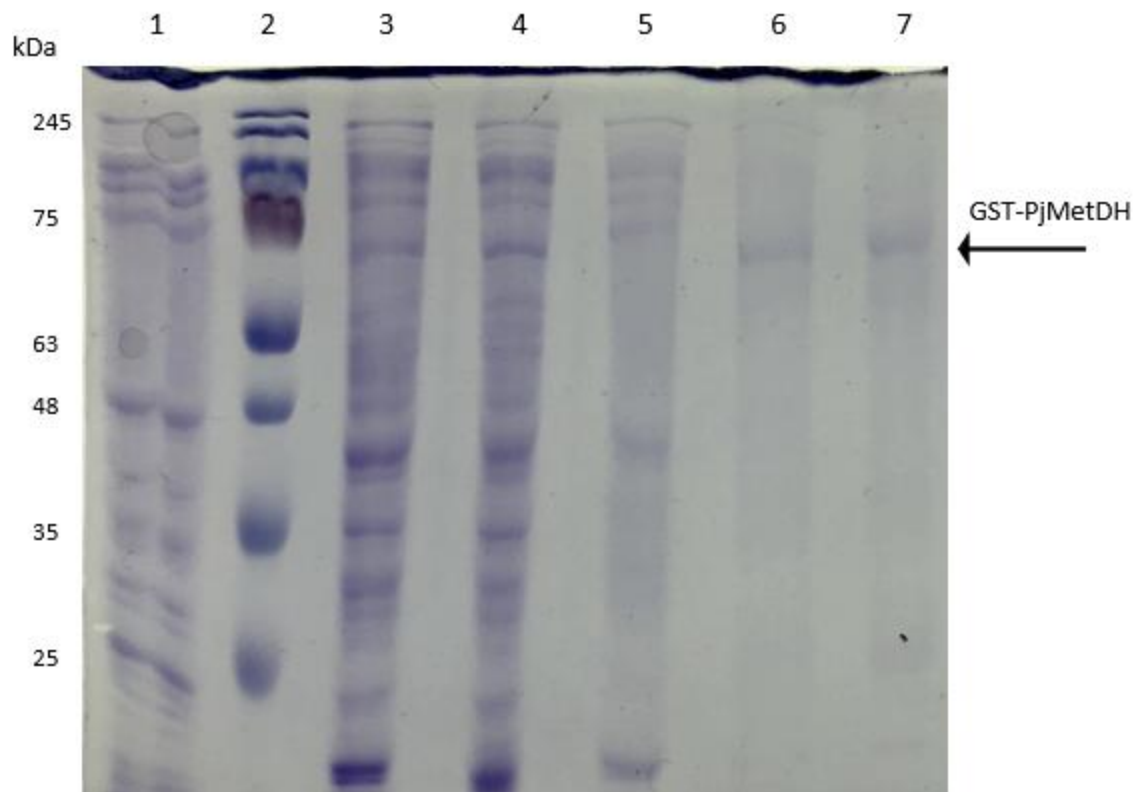


Figure 16: SDS-PAGE (10% (w/v)) gel analysis of GST-PjMetDH purification. GST-PjMetDH::pET42b/RIPL cells were grown in LB-phosphate with 50 $\mu\text{g}/\text{mL}$ kanamycin, 200 rpm, at 37°C. Protein expression was induced in cells with 500 μM IPTG for 3 hours. Purification was achieved by passing the soluble fraction over 1mL bed volume of glutathione sepharose 4 fast flow resin (GE) and eluted with 50 mM Tris-HCl, pH 8.0, 10 mM reduced glutathione. Approximately 10 μg of protein was loaded for the insoluble, soluble, NBE and wash fractions, and 2 μg of protein was loaded for the elution fractions. Lane 1: insoluble fraction; Lane 2: MBI rainbow protein molecular weight ladder; Lane 3: soluble fraction; Lane 4: non-binding eluate (NBE); Lane 5: wash fraction; Lane 6: elution fraction 1; Lane 7: elution fraction 2. The SDS-PAGE gel was stained in Coomassie Brilliant Blue R-250 overnight with agitation.

Generally, before enzyme characterization can occur for fusion proteins with this GST tag, the tag must be cleaved (GE Healthcare). In the case of the GST-PjMetDH protein, the GST tag was successfully cleaved using the serine protease thrombin. The optimal time at which the GST-PjMetDH protein should be incubated with the thrombin protease was determined and the results are shown in figure 17. The optimal cleavage time was determined by incubating the GST-PjMetDH protein with the thrombin protease over a 24-hour time period, taking aliquots of the reaction mixture at the 6 time points shown below and comparing them. In figure 17, the protein band believed to represent the GST-PjMetDH protein can clearly be seen at 0, 1 and 2 hours, however after the 2-hour time point becomes indistinguishable from the surrounding contaminating proteins. The reaction time of 3 hours was determined to be optimal for GST-PjMetDH cleavage. Other important results from figure 17 include the presence of protein band at around 26kDa in all time points including the 0-hour point. This band represents the GST portion of the fusion protein. As well, in all samples excluding the 0-hour sample, a protein band at approximately the expected molecular weight of the PjMetDH protein, 44 kDa is present. The staining process used in figure 17 differs from that of figure 16 as the Coomassie Brilliant Blue staining method was not adequately sensitive to detect samples, therefore we opted for a more sensitive staining method, using the SYPRO Ruby protein gel stain.

Following successful cleavage of the GST tag from the PjMetDH protein, an initial enzyme activity assay was performed on the cleaved but unseparated GST and PjMetDH mixture, screening for all 4 amino acids, both cofactors, at pH 10.5. Results from these assays yielded no activity (results not shown).

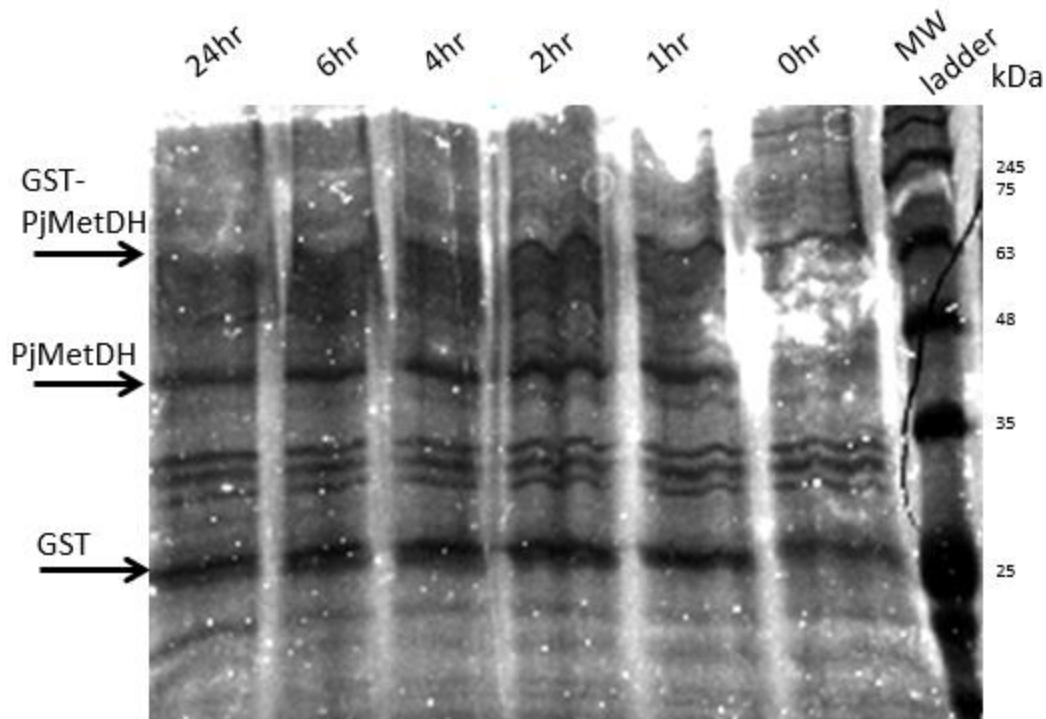


Figure 17: SDS-PAGE (10% (w/v)) gel analysis of the thrombin cleavage time trial of GST-PjMetDH. GST-PjMetDH was harvested from *E. coli* RIPL cells. The soluble fraction was purified over a 1mL bed volume of glutathione Sepharose 4 fast flow resin (GE) and eluted with 50 mM Tris-HCl, pH 8.0, 10 mM reduced glutathione. Protein eluants were combined and desalted into 1X PBS. The digest reaction was carried out at a ratio of 30 U thrombin/1000 μ g protein. 2 μ g of protein was taken from each time point (0, 1, 2, 4, 6, 24 hour). The gel was stained in SYPRO Ruby protein gel stain. The molecular weight ladder used was the MBI rainbow protein molecular weight ladder. The predicted protein bands for GST-PjMetDH, cleaved PjMetDH and GST are indicated on the figure.

Protein expression trial 2

The second protein expression trial resulted in a much higher yield of the GST-PjMetDH protein compared to the first. In trial 1, the amount of GST-PjMetDH measured following the GSH affinity column purification step was 112 μ g while the second trial yielded 2.2 mg of the GST-PjMetDH protein. Although some contaminating proteins can be seen upon SDS-PAGE gel analysis as seen in figures 16, 17 and 18, the most abundant protein is the GST-PjMetDH protein. The comparison of all the completed purification steps of the second protein expression trial are presented. Beginning with the insoluble fraction, followed by the soluble, non-binding eluate, wash and elution fractions, then the 0, 1- and 2-hour

thrombin cleavage. Comparing lane 6 which contains the purified GST-PjMetDH fraction to lanes 7 through 9, it can be observed that the protein bands at approximately 70kDa is visible in each of these samples, as well as the 26 kDa GST protein, the 44 kDa PjMetDH protein is not visible in the purified fraction, nor is it present in the 0-hour fraction. A band at the expected 44k Da range does appear at the 1-hour mark and is also present in the 2-hour time point.

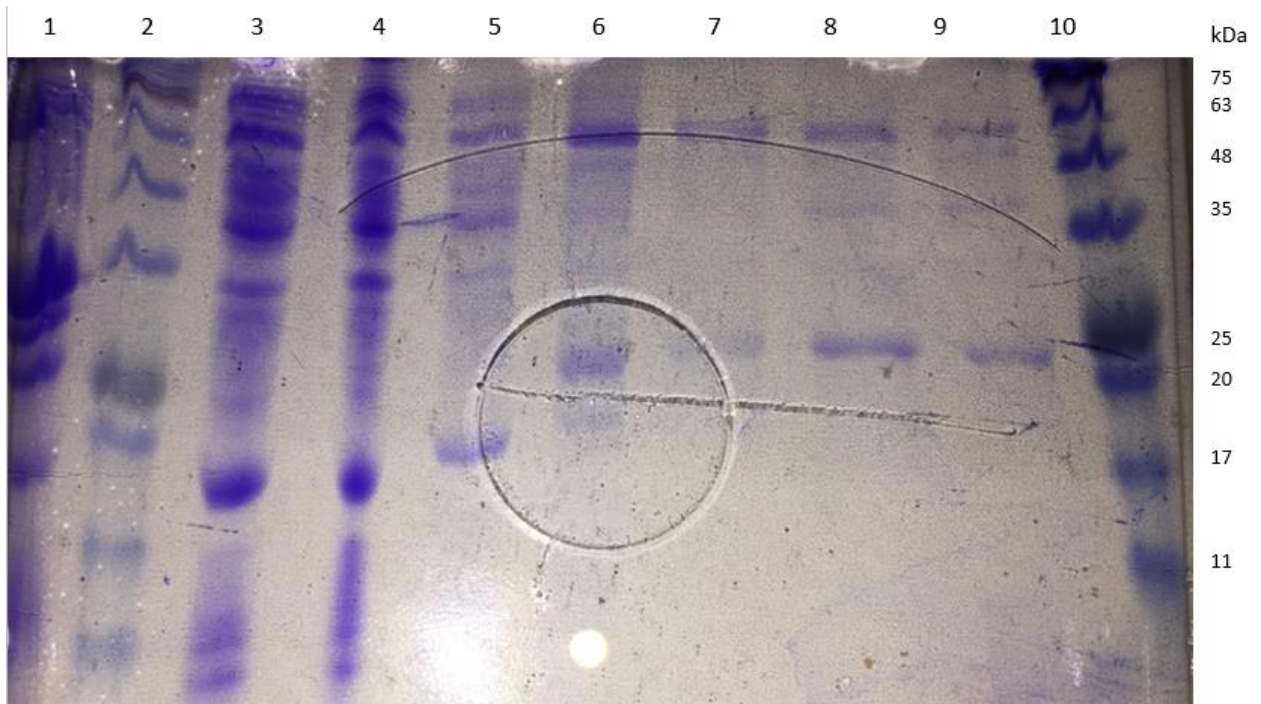


Figure 18: SDS-PAGE (10% (w/v)) gel analysis of GST-PjMetDH purification. GST-PjMetDH::pET42b/RIPL cells were grown in LB-phosphate with 50 $\mu\text{g}/\text{mL}$ kanamycin, 200 rpm, at 37°C. Protein expression was induced in cells with 500 μM IPTG overnight. Purification was achieved by passing the soluble fraction over 1mL bed volume of glutathione Sepharose 4 fast flow resin (GE) and eluted with 50 mM Tris-HCl, pH 8.0, 10 mM reduced glutathione. Lane 1: insoluble fraction; Lane 2: MBI rainbow protein molecular weight ladder; Lane 3: soluble fraction; Lane 4: non-binding eluate (NBE); Lane 5: wash fraction ; Lane 6: elution fraction 1; Lane 7: 0hr thrombin cleavage; Lane 8: 1hr thrombin cleavage; Lane 9: 2hr thrombin cleavage; Lane 10: MBI rainbow protein molecular weight ladder. The gel was stained in Coomassie Brilliant Blue R-250 overnight with agitation.

Further purification of the PjMetDH protein by passing the cleaved GST and PjMetDH mixture over another glutathione affinity column could not be completed due to solubility issues. Following the elution of the GST-PjMetDH from the GSH affinity column in the first round of purification, protein precipitated out onto all membranes used thereafter. This prevented the removal of excess free reduced glutathione which must be removed from samples prior to passing them over the GSH affinity column. Membranes on which the protein precipitated onto include the NanoSep concentrator as well as the frit portion of the Econo-Pac[®] 10DG desalting column. A final attempt at desalting the PjMetDH and GST mixture was completed via a PIERCE Slide-A-Lyzer[®] dialysis cassette. To measure the effectiveness of the dialysis procedure at removing the glutathione, a glutathione colorimetric assay was performed. The results presented in table 1 show a 244-fold reduction in detectable free glutathione in the post-dialysis sample compared to the pre-dialysis sample.

Table 1: Glutathione colorimetric assay. Free reduced glutathione was measured by incubating samples with 0.1 mM DTNB, 0.1 M Tris-HCl, pH 7.5 for 2 minutes and measuring absorbance at 412 nm.

Sample	Absorbance at 412 nm	Concentration free reduced glutathione (mM)
Pre-dialysis	0.12100	0.171
Post-dialysis	0.00100	0.0007067

Discussion

Bioinformatic analysis, including phylogenetic relationship between the PjMetDH protein sequence, as well as protein sequence alignments show that there is evidence to support the hypothesis that this putative *Polysiphonia* methionine dehydrogenase is an amino acid dehydrogenase and belongs to the Glu/Leu/Phe/Val (ELFV) dehydrogenase family. The neighbour-joining phylogenetic tree (figure 6) shows the PjMetDH protein as being more closely related to the Glu/Leu/Phe/Val (ELFV) family of dehydrogenases, rather than another dehydrogenase subclass such as alcohol dehydrogenases which act on the CH-OH group of the substrate, as does histidinol dehydrogenase (Eccleston *et al.*, 1979).

Furthermore, many important structural and catalytic amino acid residues which have been found to be highly conserved in many amino acid dehydrogenases have been identified in PjMetDH (figure 7). A critical lysine residue, Lys68, which in 1994 Sekimoto *et al.* demonstrated was present in most amino acid dehydrogenases is present in PjMetDH. Sekimoto *et al.* concluded that the Lys68 residue was found in the active site of the enzyme and was critical for proper substrate binding. Prior to the identification of this critical Lys68 residue, the same research group identified another critical lysine residue, Lys80 which they demonstrated also has a role in catalysis and is also conserved in many amino acid dehydrogenases (Matsuyama *et al.*, 1992; Sekimoto *et al.*, 1993). This Lys80 can also be identified in PjMetDH. Many amino acid residues involved in cofactor binding have been identified in amino acid dehydrogenases by many researcher (Baker *et al.*, 1995; Chen and Engel, 2009; Sekimoto *et al.*, 1994; Yamaguchi *et al.*, 2019). These include Gly77(○), Gly78 (●), Ser147(β), Gln179(¶), Gly180(ϕ), Val204(×), Isoleucine204 (-), Ala238 (§), Leu239 (∅), Ser259 (÷), Asn261 (δ) and Gly290 (θ). All the listed amino acid residues were found to be conserved with either identical residues or residues with similar properties aside from Gly79 and Gly290. Mutagenesis studies have identified residues that when substituted, either increase or decrease an amino acid dehydrogenases activity towards methionine. Examples of these include Gly124(α) and Leu304(λ) identified by Seah *et al.* in 1995 and 2003. The researchers substituted the glycine at position 124 to alanine, and leucine at position 304 to valine in the *Bacillus sphaericus* phenylalanine dehydrogenase and found that the single G124A mutant and the G124;L304V double mutant showed shifts in activity towards *L*-methionine. The present

study found that the protein sequence for PjMetDH had a valine residue at the corresponding Leu304 position and a glycine at the G124 position. Having certain amino acid residues at key positions such as valine at position 304 which has been shown to shift the activity of phenylalanine dehydrogenase towards methionine suggests that the putative methionine dehydrogenase of the present study may also have activity toward methionine.

Of the three target PjMetDH constructs with which cloning was attempted, a single construct, the GST-PjMetDH::pET42b variation was successfully cloned, expressed and partially purified. While attempting to clone the two unsuccessful construct, self-ligation and false positive clones were frequently recorded (figures 10 and 14). The issue of self-ligation was resolved by dephosphorylating the restriction endonuclease digested vectors, effectively preventing the overhangs from self ligating (Figure 11, 12 and 13). However, based on the sequencing results it seems that contamination had occurred at some step as the gene insert which was believed to be PjMetDH was determined to be the *U. mutabilis* MOTB reductase gene. This gene was previously cloned by the Waller lab group and makes up part of the *U. mutabilis* DMSP synthetase. This indicates that contamination occurred at some point. To prevent further complications with producing construct variants it would be favourable to have the two unsuccessfully cloned constructs synthesized as was the GST-PjMetDH::pET42b construct.

We demonstrate that protein expression of GST-PjMetDH is optimized with a longer protein expression time, a value originally set at 3 hours which was extended to approximately 18 hours or overnight. These changes, along with the doubling of the day culture volume increased GST-PjMetDH protein yield from 112 µg to 2.2mg. The purification methods completed in the present study were successful, in figures 15-18 comparisons of various purification stages can be observed. The presence of a protein band at the expected molecular weight of the GST-PjMetDH protein in the insoluble protein fraction indicates that there was likely loss of protein at that stage. When visually comparing the insoluble, soluble, nonbinding eluate and wash stages of purification, contaminating proteins can be observed decreasing in number with increasing purification stage. The GST affinity tag was successfully cleaved from the PjMetDH portion of the fusion protein seen in figure 17. An interesting finding of the thrombin cleavage trial was the presence of what is believed to be the GST tag in the 0-hour

sample. This is an interesting finding as at the 0-hour mark, the thrombin protease would not have had sufficient time to cleave any of the affinity tag from the fusion protein, leading to a frameshift and a premature stop codon, as has been seen with other recombinant GST-fusion protein (J.C. Waller, unpublished observation).

Solubility issues were encountered following the elution of the GST-PjMetDH protein from the GSH affinity column with 50 mM Tris-HCl, pH 8.0, 10 mM reduced glutathione. The eluted protein could not be desalted as it precipitated onto membranes such as those found in centrifugal concentrators, desalting columns and dialysis cassettes, preventing the completion of the final purification steps. Final purification steps would have involved passing the cleaved PjMetDH protein over a GSH affinity column which would have removed the cleaved GST from solution. Three desalting methods were attempted including the usage of centrifugal concentrators, desalting columns, and dialysis cassettes but none were successful.

Enzyme activity assays were completed on the impure, cleaved PjMetDH protein (results not shown). This initial investigation into the activity of the methionine dehydrogenase resulted in no noticeable activity. It was initially believed that the reaction was going to completion much more quickly than could be detected by the equipment and technique employed, therefore trials using less protein were attempted. These also yielded negative results as no activity was recorded. There are many possible explanations as to why enzyme activity was not observed. Firstly, contaminating proteins such as the cleaved GST tag or other as seen in figure 17 could have interfered with the methionine dehydrogenase and prevented proper catalysis. Secondly, all activity assays were completed at pH 10.5, a value taken from a similar study by Yamasaki-Yashiki *et al.* in 2012 where researchers selectively mutated amino acid residues of a phenylalanine dehydrogenase to shift its activity towards methionine. The enzyme activity assay conditions described by Yamasaki-Yashiki *et al.* were employed in the present study, however it is possible that the putative methionine dehydrogenase does not have activity at this pH.

Future directions

Future research directions involving the study of this putative methionine dehydrogenase include resolving the solubility issues encountered herein. This may be accomplished by optimizing the separation techniques used in the separation of the cleaved GST-PjMetDH as well as optimizing the buffers used in these processes. Another avenue for solving the solubility issues should include the cloning, expression and purification of the two constructs; PjMetDH-H₆::pET28b and NUS-PjMetDH::pET44a, which could not be successfully cloned in this study.

Once successful cloning, expression and purification has been achieved for one of the three PjMetDH constructs, further investigation into the enzyme activity of the impure, cleaved PjMetDH protein should also be completed. Particularly in investigating a pH range between pH 6 and 10.5, but also including the determination of substrate and cofactor specificities. Following proper enzymatic characterization of the putative methionine dehydrogenase, it would be interesting to compare the recombinant methionine dehydrogenase activity to methionine dehydrogenase activity from *Polysiphonia lanosa* tissues samples.

DMSP biosynthesis seems to be a very streamlined process, and it would be unfavourable for organisms to invest an excess of the starting material methionine into this pathway, especially under unfavourable conditions. Therefore, a future direction could involve determining if downstream metabolites of the DMSP pathways such as MTOB, MTHB, or others have the capacity inhibit methionine dehydrogenase activity.

Further research into this putative methionine dehydrogenase will expand current knowledge of the DMSP biosynthetic pathway in algal species as it is poorly understood in species outside of *U. mutabilis*.

References

- Andreae, M.O., 1990. Ocean-atmosphere interactions in the global biogeochemical sulfur cycle. *Mar. Chem.* 30, 1–29.
- Baker, P.J., Turnbull, A.P., Sedelnikova, S.E., Stillman, T.J., Rice, D.W., 1995. A role for quaternary structure in the substrate specificity of leucine dehydrogenase. *Structure* 3, 693–705.
- Blunden, G., Smith, B.E., Irons, M.W., Yang, M.-H., Roch, O.G., Patel, A.V., 1992. Betaines and tertiary sulphonium compounds from 62 species of marine algae. *Biochem. Syst. Ecol.* 20, 373–388.
- Bradford, M.M., 1976. A rapid and sensitive method for the quantitation of microgram quantities of protein utilizing the principle of protein-dye binding. *Anal. Biochem.* 72, 248–254.
- Brunhuber, N.M., Blanchard, J.S., 1994. The biochemistry and enzymology of amino acid dehydrogenases. *Crit. Rev. Biochem. Mol. Biol.* 29, 415–467.
- Challenger, F., Simpson, M.I., 1947. A precursor of the dimethyl sulphide evolved by *Polysiphonia fastigiata*; dimethyl-beta-propiothetine (dimethyl-beta-carboxyethylsulphonium hydroxide) and its salts. *Biochem. J.* 41, xl.
- Chen, S., Engel, P.C., 2009. Efficient screening for new amino acid dehydrogenase activity: directed evolution of *Bacillus sphaericus* phenylalanine dehydrogenase towards activity with an unsaturated non-natural amino acid. *J. Biotechnol.* 142, 127–134.
- Chillemi, R., Patti, A., Morrone, R., Piattelli, M., Sciuto, S., 1990. The Role of Methylsulphonium Compounds in the Biosynthesis of N-Methylated Metabolites in *Chondria coerulescens*. *J. Nat. Prod.* 53, 87–93.
- Curson, A.R.J., Liu, J., Bermejo Martínez, A., Green, R.T., Chan, Y., Carrión, O., Williams, B.T., Zhang, S.-H., Yang, G.-P., Bulman Page, P.C., Zhang, X.-H., Todd, J.D., 2017. Dimethylsulfoniopropionate biosynthesis in marine bacteria and identification of the key gene in this process. *Nat. Microbiol.* 2, 17009.
- Dickson, D.M.J., Kirst, G.O., 1987. Osmotic Adjustment in Marine Eukaryotic Algae: The Role of Inorganic Ions, Quaternary Ammonium, Tertiary Sulphonium and Carbohydrate Solutes. II. Prasinophytes and Haptophytes. *New Phytol.* 106, 657–666.
- Eccleston, E.D., Thayer, M.L., Kirkwood, S., 1979. Mechanisms of action of histidinol dehydrogenase and UDP-Glc dehydrogenase. Evidence that the half-reactions proceed on separate subunits. *J. Biol. Chem.* 254, 11399–11404.
- Eyer, P., Worek, F., Kiderlen, D., Sinko, G., Stuglin, A., Simeon-Rudolf, V., Reiner, E., 2003. Molar absorption coefficients for the reduced Ellman reagent: reassessment. *Anal. Biochem.* 312, 224–227.
- Gage, D.A., Rhodes, D., Nolte, K.D., Hicks, W.A., Leustek, T., Cooper, A.J.L., Hanson, A.D., 1997. A new route for synthesis of dimethylsulphonioacetate in marine algae. *Nature* 387, 891–894.
- Hanson, A.D., Gage, D.A., 1996. 3-Dimethylsulfoniopropionate Biosynthesis and use by Flowering Plants, in: Kiene, R.P., Visscher, P.T., Keller, M.D., Kirst, G.O. (Eds.), *Biological and Environmental Chemistry of DMSP and Related Sulfonium Compounds*. Springer US, Boston, MA, pp. 75–86.

- Hanson, A.D., Rivoal, J., Paquet, L., Gage, D.A., 1994. Biosynthesis of 3-dimethylsulfoniopropionate in *Wollastonia biflora* (L.) DC. Evidence that S-methylmethionine is an intermediate. *Plant Physiol.* 105, 103–110.
- Howarth, R.W., 1984. The ecological significance of sulfur in the energy dynamics of salt marsh and coastal marine sediments. *Biogeochemistry* 1, 5–27.
- Husband, J.D., Kiene, R.P., Sherman, T.D., 2012. Oxidation of dimethylsulfoniopropionate (DMSP) in response to oxidative stress in *Spartina alterniflora* and protection of a non-DMSP producing grass by exogenous DMSP+acrylate. *Environ. Exp. Bot.* 79, 44–48.
- Jørgensen, B.B., Findlay, A.J., Pellerin, A., 2019. The Biogeochemical Sulfur Cycle of Marine Sediments. *Front. Microbiol.* 10, 849
- Keller, M.D., Kiene, R.P., Matrai, P.A., Bellows, W.K., 1999. Production of glycine betaine and dimethylsulfoniopropionate in marine phytoplankton. I. Batch cultures. *Mar. Biol.* 135, 237–248.
- Kocsis, M.G., Nolte, K.D., Rhodes, D., Shen, T.L., Gage, D.A., Hanson, A.D., 1998. Dimethylsulfoniopropionate biosynthesis in *Spartina alterniflora*. Evidence that S-methylmethionine and dimethylsulfoniopropylamine are intermediates. *Plant Physiol.* 117, 273–281.
- Ksionzek, K.B., Lechtenfeld, O.J., McCallister, S.L., Schmitt-Kopplin, P., Geuer, J.K., Geibert, W., Koch, B.P., 2016. Dissolved organic sulfur in the ocean: Biogeochemistry of a petagram inventory. *Science* 354, 456–459.
- Laemmli, U.K., 1970. Cleavage of structural proteins during the assembly of the head of bacteriophage T4. *Nature* 227, 680–685.
- Lovelock, J.E., Maggs, R.J., Rasmussen, R.A., 1972. Atmospheric Dimethyl Sulphide and the Natural Sulphur Cycle. *Nature* 237, 452.
- Malin, G., 1996. The Role of DMSP and DMS in the Global Sulfur Cycle and Climate Regulation, in: Kiene, R.P., Visscher, P.T., Keller, M.D., Kirst, G.O. (Eds.), *Biological and Environmental Chemistry of DMSP and Related Sulfonium Compounds*. Springer US, Boston, MA, pp. 177–189.
- Matsuyama, T., Soda, K., Fukui, T., Tanizawa, K., 1992. Leucine dehydrogenase from *Bacillus stearothermophilus*: identification of active-site lysine by modification with pyridoxal phosphate. *J. Biochem.* 112, 258–265.
- Mifflin, B.J., Habash, D.Z., 2002. The role of glutamine synthetase and glutamate dehydrogenase in nitrogen assimilation and possibilities for improvement in the nitrogen utilization of crops. *J. Exp. Bot.* 53, 979–987.
- Otte, M.L., Wilson, G., Morris, J.T., Moran, B.M., 2004. Dimethylsulphoniopropionate (DMSP) and related compounds in higher plants. *J. Exp. Bot.* 55, 1919–1925.
- Robinson, E., Robbins, R.C., 1972. Emissions, concentrations, and fate of gaseous atmospheric pollutants, 2nd ed, Air pollution control. Wiley-Interscience, New York.
- Seah, S.Y., Britton, K.L., Baker, P.J., Rice, D.W., Asano, Y., Engel, P.C., 1995. Alteration in relative activities of phenylalanine dehydrogenase towards different substrates by site-directed mutagenesis. *FEBS Lett.* 370, 93–96.
- Seah, S.Y.K., Britton, K.L., Rice, D.W., Asano, Y., Engel, P.C., 2003. Kinetic analysis of phenylalanine dehydrogenase mutants designed for aliphatic amino acid dehydrogenase activity with guidance from homology-based modelling. *Eur. J. Biochem.* 270, 4628–4634.

- Sekimoto, T., Fukui, T., Tanizawa, K., 1994. Involvement of conserved lysine 68 of *Bacillus stearothermophilus* leucine dehydrogenase in substrate binding. *J. Biol. Chem.* 269, 7262–7266.
- Sekimoto, T., Matsuyama, T., Fukui, T., Tanizawa, K., 1993. Evidence for lysine 80 as general base catalyst of leucine dehydrogenase. *J. Biol. Chem.* 268, 27039–27045.
- Slatt, B.J., Natusch, D.F.S., Prospero, J.M., Savoie, D.L., 1978. Hydrogen sulfide in the atmosphere of the northern equatorial Atlantic Ocean and its relation to the global sulfur cycle. *Atmospheric Environ.* 1967 12, 981–991.
- Stefels, J., 2000. Physiological aspects of the production and conversion of DMSP in marine algae and higher plants. *J. Sea Res.* 43, 183–197.
- Summers, P.S., Nolte, K.D., Cooper, A.J.L., Borgeas, H., Leustek, T., Rhodes, D., Hanson, A.D., 1998. Identification and Stereospecificity of the First Three Enzymes of 3-Dimethylsulfoniopropionate Biosynthesis in a Chlorophyte Alga. *Plant Physiol.* 116, 369–378.
- Taylor, B.F., Gilchrist, D.C., 1991. New routes for aerobic biodegradation of dimethylsulfoniopropionate. *Appl. Environ. Microbiol.* 57, 3581–3584.
- Trossat, C., Nolte, K.D., Hanson, A.D., 1996. Evidence That the Pathway of Dimethylsulfoniopropionate Biosynthesis Begins in the Cytosol and Ends in the Chloroplast. *Plant Physiol.* 111, 965–973.
- Vroon, D.H., Israili, Z., 1990. Aminotransferases, 3rd ed, Clinical method: The History, Physical, and Laboratory Examinations. Butterworths, Boston.
- Wang, X.G., Britton, K.L., Stillman, T.J., Rice, D.W., Engel, P.C., 2001. Conversion of a glutamate dehydrogenase into methionine/norleucine dehydrogenase by site-directed mutagenesis. *Eur. J. Biochem.* 268, 5791–5799.
- Yamaguchi, H., Kamegawa, A., Nakata, K., Kashiwagi, T., Mizukoshi, T., Fujiyoshi, Y., Tani, K., 2019. Structural insights into thermostabilization of leucine dehydrogenase from its atomic structure by cryo-electron microscopy. *J. Struct. Biol.* 205, 11–21.
- Yamasaki-Yashiki, S., Tachibana, S., Asano, Y., 2012. Determination of L-methionine using methionine-specific dehydrogenase for diagnosis of homocystinuria due to cystathionine β -synthase deficiency. *Anal. Biochem.* 428, 143–149.
- Yoch, D.C., 2002. Dimethylsulfoniopropionate: Its Sources, Role in the Marine Food Web, and Biological Degradation to Dimethylsulfide. *Appl. Environ. Microbiol.* 68, 5804–5815.
- Zeller, E.A., Maritz, A., 1944. Über eine neue l-Aminosäure-oxydase. (1. Mitteilung). *Helv. Chim. Acta* 27, 1888–1902.
- Zor, T., Selinger, Z., 1996. Linearization of the Bradford protein assay increases its sensitivity: theoretical and experimental studies. *Anal. Biochem.* 236, 302–308.